Group 4 Metal Complexes of Nitrogen-Bridged Dialkoxide Ligands: Synthesis, Structure, and Polymerization Activity Studies

Laurent Lavanant,[†] Loic Toupet,[‡] Christian W. Lehmann,[§] and Jean-François Carpentier*,[†]

Organométalliques et Catalyse, UMR 6509 CNRS-Université de Rennes 1, Institut de Chimie de Rennes, 35042 Rennes Cedex, France, Groupe Matière Condensée et Matériaux, Cristallochimie, UMR 6626 CNRS-Université de Rennes 1, 35042 Rennes Cedex, France, and Max-Planck-Institut für Kohlenforschung, Chemical Crystallography, Postfach 101353, 45466 Mülheim/Ruhr, Germany

Received July 12, 2005

Neutral soluble titanium(IV) and zirconium(IV) complexes of new amino-dialkoxide ligands $\{OCR_2CH_2N(CH_2Ph)CH_2CR_2O\}^{2-}$ ($\{ONOR\}^{2-}$) have been prepared. Alcohol and alkane elimination reactions from $\{ONOR\}H_2$ (R = Me, **1**; *p*-tol, **2**) and salt metathesis routes from $Li_2\{ONO^{Me}\}$ in situ-generated afford $\{ONO^{Me}\}Ti(OiPr)_2$ (**3**), $\{ONO^{R}\}_2M$ (R = Me, M = Ti, **5**; Zr, **6**; R = *p*-tol, M = Zr, **7**), $\{ONO^{Me}\}Zr(CH_2Ph)_2$ (**8**), $\{ONO^{Me}\}ZrCl_2(THF)_n$ (n = 0, **9**; n = 1, **10**), $\{ONO^{Me}\}Zr(NMe_2)_2$ (**11**), and $\{ONO^{R}\}TiCl_2$ (R = Me, **13**; R = *p*-tol, **14**) in good yields. X-ray crystallographic studies showed that **3**, **8**, **13**, and **14** adopt in the solid state mononuclear structures, with coordination of the nitrogen atom to the metal center. Dinuclear structures with bridging alkoxide and amido ligands were observed for **6** and a mixed amido-$\{ONO^{Me}\}Zr$ complex (**12**) isolated in the preparation of **11**. NMR data are consistent with the existence of a single monomeric species in toluene solution for all complexes, except **11** and dichlorozirconium complexes **9** and **10**, for which mixtures of monomeric and possibly aggregated species are observed in toluene and THF. The dynamic behavior of monomeric species **3**, **8**, **13**, and **14** in toluene was investigated by variable-temperature NMR spectroscopy. The activation parameters determined by line-shape analysis, in particular for **8** ($\Delta H^{\ddagger} = 20.0 \pm 1$ kcal·mol^{-1}; $\Delta S^{\ddagger} = 13.1 \pm 2$ cal·mol^{-1}·K^{-1}) and **13** ($\Delta H^{\ddagger} = 17.4 \pm 1$ kcal·mol^{-1}; $\Delta S^{\ddagger} = 11.4 \pm 2$ cal·mol^{-1}·K^{-1}), suggest a process involving dissociation of nitrogen, inversion of configuration at nitrogen, and amine re-coordination. The bulkiness of the R substituents affects the fluxional behavior of $\{ONO^{R}\}TiCl_2$ (R = Me, **13**; R = *p*-tol, **14**). The THF-free dichlorozirconium complex **9** in combination with MAO generates highly active but very unstable ethylene polymerization catalyst systems.

Introduction

Numerous examples of nonmetallocene group 4 complexes have now been reported.[1] Among these, a diverse range of complexes that contain heteroatom-bridged diaryloxide ligands $\{OZO\}^{2-}$ (e.g., Z = N, S) have been identified as promising olefin polymerization catalysts.[2,3] In these systems, the bridging heteroatom Z can provide, if coordinated, the stereochemically rigid framework essential for stereoregular polymer formation.[1] First of all, the bridging heteroatom X may also provide an increased stabilization of reactive, electron-deficient metal centers. Indeed, aryloxides ($O-C(sp^2)$) are not generally considered to contribute sufficient electron density to be isolobal to the cyclopentadienyl ligand.[1,4] This situation is more critical for alkoxides ($O-C(sp^3)$), as evidenced by the large tendency of these ligands to form aggregated structures with early transition metals.[4] Introduction of a heteroatom with additional donor functionalities into a chelating multidentate alkoxide ligand can tackle this problem.[4] However, reports of well-characterized group 4 metal complexes with multidentate dialkoxide ligand systems, such as amino-dialkoxides[5−,8] or sulfur-bridged dialkoxides,[9] are limited. Most of these systems have been used for polymerization[10] or fine chemicals catalysis,[11,12] and the exact nature of the precursors and active species remains unclear.

In this contribution, we describe a series of soluble titanium(IV) and zirconium(IV) complexes of the new tridentate amino-dialkoxide ligand systems $\{OCR_2CH_2N(CH_2Ph)CH_2CR_2O\}^{2-}$ ($\{ONOR\}^{2-}$, R = Me, *p*-tolyl). The objectives of this work were to define the $\{ONO^{R}\}^{2-}$ coordination properties in simple group 4 $\{ONOR\}MX_2$ complexes, to allow structural comparison, in the solid

* Corresponding author. Fax: (+33)(0)223-236-939. E-mail: jean-francois.carpentier@univ-rennes1.fr.
† Organométalliques et Catalyse.
‡ Groupe Matière Condensée et Matériaux.
§ Max-Planck-Institut.

(1) For reviews on post-metallocene complexes of group 4 metals, see: (a) Britovsek, G. J. P.; Gibson, V. C.; Wass, D. F. *Angew. Chem., Int. Ed.* **1999**, *38*, 428−447. (b) Coates, G. W. *J. Chem. Soc., Dalton Trans.* **2002**, 467−475. (c) Gibson, V. C.; Spitzmesser, S. K. *Chem. Rev.* **2003**, *103*, 283−315. (d) Suzuki, Y.; Terao, H.; Fujita, T. *Bull. Chem. Soc. Jpn*. **2003**, *76*, 1493−1517. (e) Corradini, P.; Guerra, G.; Cavallo, L. *Acc. Chem. Res.* **2004**, *37*, 231−241.

10.1021/om0505817 CCC: $30.25
Publication on Web 10/04/2005

state and solution, with related systems that differ in the size of chelate ring, the nature of the alkoxide carbon and nitrogen substituents, and the nature of the heteroatom.[9] The ethylene polymerization properties of $\{ONO^R\}MX_2$/MAO and $\{ONO^R\}MR^+$ in situ-generated catalysts have also been investigated.

Results and Discussion

Ligand Synthesis. Two new ligands were prepared to explore the influence of the R substituents in $\{OCR_2CH_2N(CH_2Ph)CH_2CR_2O\}^{2-}$ ligands and Ti(IV) and Zr(IV) complexes thereof. The dimethyl-substituted nitrogen−bridged diol $\{ONOMe\}H_2$ (**1**) was prepared in nearly quantitative yield via ring-opening of isobutylene oxide by benzylamine (eq 1). The *para*-tolyl-substituted diol $\{ONO^{tol}\}H_2$ (**2**) was obtained from the reaction of an excess of the *p*-tolyl Grignard reagent with the appropriate amino-diester[13] (eq 2). This route proved more efficient than the ring-opening of the diaryl-substituted oxirane $(p\text{-tol})_2\overset{\frown}{COCH_2}$ (2−5 equiv) by benzylamine, which yielded only the 1:1 amino-alcohol product $(p\text{-tol})_2C(OH)CH_2NHCH_2Ph$. Both diols **1** and **2** were obtained as microcrystalline powders.

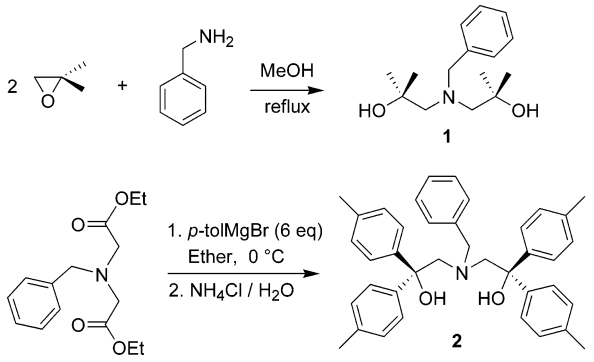

Synthesis of Neutral Complexes. Several routes to $\{ONO^R\}$-Ti and $\{ONO^R\}$-Zr complexes have been explored: (a) σ-bond metathesis reactions between the diols and an appropriate homoleptic metal precursor enabling either alkane, alcohol, or amine elimination; (b) salt elimination reactions between the $Li_2\{ONO^{Me}\}$ salt in situ-generated and $MCl_4(THF)_n$. These results are summarized in Schemes 1 and 2 and eq 3. The prepared neutral complexes are all air- and moisture-sensitive and were characterized in the solid state by elemental analysis and X-ray diffraction studies for some of them, and in solution by variable-temperature ^1H and ^{13}C NMR spectroscopy (vide infra).

The 1:1 σ-bond metathesis reaction of diol **1** and $Ti(OiPr)_4$ proceeded readily and selectively to yield $\{ONO^{Me}\}Ti(OiPr)_2$ (**3**) (Scheme 1). Attempts to prepare the parent zirconium complex $\{ONO^{Me}\}Zr(OtBu)_2$ (**4**) with $Zr(OtBu)_4$ and **1** under various conditions invariably yielded mixtures of **4** and the bis-ligand complex $\{ONO^{Me}\}_2Zr$ (**6**), which could not be separated by recrystallization.[14] Both **6** and the analogous titanium complex **5** were prepared efficiently by the reaction of 2 equiv of **1** with $M(OR)_4$ complexes. Similar reaction with the *p*-tolyl-substituted diol **2** afforded the parent bis-ligand zirconium complex $\{ONO^{tol}\}_2Zr$ (**7**) in quantitative yield. Complex **6** served as an efficient entry to the dibenzyl complex $\{ONO^{Me}\}Zr(CH_2Ph)_2$ **8** via comproportionation with $Zr(CH_2Ph)_4$. Alcoholysis of $Zr(CH_2Ph)_4$ with **1** affords a more direct and easier synthesis of **8**.

(2) For examples see: (a) Kakugo, M.; Miyatake, T.; Mizunuma, K. *Chem. Express.* **1987**, *2*, 445−448. (b) Miyatake, T.; Mizunuma, K.; Seki, Y.; Kakugo, M. *Macromol, Rapid Commun.* **1989**, *10*, 349−352. (c) Van der Linden, A.; Schaverien, C. J.; Meiboom, N.; Ganter, C.; Orpen, A. G. *J. Am. Chem. Soc.* **1995**, *117*, 3008−3021. (c) Tshuva, E. Y.; Goldberg, I.; Kol, M. *J. Am. Chem. Soc.* **2000**, *122*, 10706−10707. (d) Tshuva, E. Y.; Goldberg, I.; Kol, M. *Inorg. Chem.* **2001**, *40*, 4263−4270. (e) Tshuva, E. Y.; Goldberg, I.; Kol, M., Goldschmidt, Z. *Organometallics* **2001**, *20*, 3017−3028. (f) Tshuva, E. Y.; Goldberg, I.; Kol, M.; Goldschmidt, Z. *Chem. Commun.* **2001**, 2120−2121. (g) Tshuva, E. Y.; Groysman, S.; Goldberg, I.; Kol, M.; Goldschmidt, Z. *Organometallics* **2002**, *21*, 662−670. (h) Balsells, J.; Carroll, P. J.; Walsh, P. J. *Inorg. Chem.* **2001**, *40*, 5568−5574. (i) Tian, J. P.; Hustad, D.; Coates, G. W. *J. Am. Chem. Soc.* **2001**, *123*, 5134−5135. (j) Boyd, C. L.; Toupance, T.; Tyrell, B. R.; Ward, B. D.; Wilson, C. R.; Cowley, A. R.; Mountford, P. *Organometallics* **2005**, *24*, 309−330. (k) Toupance, T.; Dubberley, S. R.; Rees, N. H.; Tyrrell, B. R.; Mountford, P. *Organometallics* **2002**, *21*, 1367−1382. (l) Fokken, S.; Spaniol, T. P.; Kang, H.-C.; Massa, W.; Okuda, J. *Organometallics* **1996**, *15*, 5069−5072. (m) Sernetz, F. G.; Muelhaupt, R.; Fokken, S.; Okuda, J. *Macromolecules* **1997**, *30*, 1562−1569. (n) Capacchione, C.; Proto, A.; Ebeling, H.; Mülhaupt, R.; Möller, K.; Spaniol, T. P.; Okuda, J. *J. Am. Chem. Soc.* **2003**, *125*, 4964−4965. (o) Natrajan, L. S.; Wilson, C.; Okuda, J.; Arnold, P. L. *Eur. J. Inorg. Chem.* **2004**, 3724−3732. (p) Capacchione, C.; Manivannan, R.; Barone, M.; Beckerle, K.; Centore, R.; Oliva, L.; Proto, A.; Tuzi, A.; Spaniol, T. P.; Okuda, J. *Organometallics* **2005**, *24*, 2971−2982. (q) Takashima, Y.; Nakayama, Y.; Hirao, T.; Yasuda, H.; Harada, A. *J. Organomet. Chem.* **2004**, *689*, 612−619. (r) Janas, S.; Jerzykiewicz, L. B.; Przybylak, K.; Sobota, P.; Sczzegot, K.; Wisniewska, D. *Eur. J. Inorg. Chem.* **2004**, 1639−1645. (s) Janas, S.; Jerzykiewicz, L. B.; Przybylak, K.; Sobota, P.; Sczzegot, K.; Wisniewska, D. *Eur. J. Inorg. Chem.* **2005**, 1063−1070.

(3) For theoretical studies on $[(2\text{-}C_6H_4O)X(2'\text{-}C_6H_4O)]TiMe^+$ (X = O, S, Se, Te) systems, see: (a) Froese, R. D. F.; Musaev, D. G.; Matsubara, T.; Morokuma, K. *J. Am. Chem. Soc.* **1997**, *119*, 7190−7196. (b) Froese, R. D. F.; Musaev, D. G.; Morokuma, K. *Organometallics* **1999**, *18*, 373−379.

(4) (a) Bradley, D. C.; Mehrotra, R. M.; Rothwell, I. P.; Singh, A. *Alkoxo and Aryloxo Derivatives of Metals*; Academic Press: London, 2001. (b) Mehrotra, R. M.; Singh, A. *Prog. Inorg. Chem.* **1997**, *46*, 239−545. (c) Hubert-Pfalzgraf, L. G. *Coord. Chem. Rev.* **1998**, *178−180*, 967−997.

(5) Mack, H.; Eisen, M. *J. Chem. Soc., Dalton Trans.* **1998**, 917−921.

(6) (a) Shao, P.; Gendron, R. A. L.; Berg, D. J.; Bushnell, G. W. *Organometallics* **2000**, *19*, 509−520. (b) Shao, P.; Gendron, R. A. L.; Berg, D. J. *Can. J. Chem.* **2000**, *78*, 255−264.

(7) Gauvin, R. M.; Osborn, J. A.; Kress, J. *Organometallics* **2000**, *19*, 2944−2946.

(8) Lavanant, L.; Chou, T.-Y.; Chi, Y.; Lehmann, C. W.; Toupet, L.; Carpentier, J.-F. *Organometallics* **2004**, *23*, 5450−5458.

(9) Related group 4 sulfur-bridged dialkoxo complexes derived from the parent sulfur-bridged ligand system $\{OCR_2CH_2SCH_2CR_2O\}^{2-}$ ($\{OSO^R\}^{2-}$, R = Me, *p*-tolyl) have also been prepared. Lavanant, L.; Silvestru, A.; Faucheux, A.; Toupet, L.; Jordan, R. F.; Carpentier, J.-F. *Organometallics* **2005**, *24*, 5604−5619.

(10) (a) Manivannan, R.; Sundararajan, G. *Macromolecules* **2002**, *35*, 7883−7890. (b) Manivannan, R.; Sundararajan, G.; Kaminsky, W. *J. Mol. Catal. A: Chem.* **2000**, *160*, 85−95. (c) Carone, C.; de Lima, V.; Albuquerque, F.; Nunes, P.; de Lemos, C.; dos Santos, J. H. Z.; Galland, G. B.; Stedile, F. C.; Einloft, S.; de S. Basso, N. R. *J. Mol. Catal. A: Chem.* **2004**, *208*, 285−290.

(11) For use of amino- and pyridine-dialkoxide group 4 complexes, see: (a) Manickam, G.; Sundararajan, G. *Tetrahedron: Asymmetry* **1999**, *10*, 2913−2925. (b) Sundararajan, G.; Prabagaran, N.; Varghese, B. *Org. Lett.* **2001**, *3*, 1973−1976. (c) Hawkins, J. M. H.; Sharpless, B. *Tetrahedron Lett.* **1987**, *28*, 2825−2828. (d) Zambrano, C. H.; McMullen, A. K.; Kobriger, L. M., Fanwick, P. E.; Rothwell, I. P. *J. Am. Chem. Soc.* **1990**, *112*, 6565−6570.

(12) Leading references for use of simple (without heteroatom bridge) dialkoxide group 4 complexes: (a) Bachand, B.; Wuest, D. *Organometallics* **1991**, *10*, 2015−2025. (b) Duthaler, R. O.; Hafner, A. *Chem. Rev.* **1992**, *92*, 807−832. (c) Gothelf, K. V.; Jorgensen, A. *J. Organomet. Chem.* **1994**, *59*, 5687−5691. (d) Yamasaki, S.; Kanai, M.; Shibasaki, M. *J. Am. Chem. Soc.* **2001**, *123*, 1256−1257. (f) Ackermann, L.; Bergman, R. G.; Loy, R. N. *J. Am. Chem. Soc.* **2003**, *125*, 11956−11963.

(13) Cook, C. J.; Topich, J. *Inorg. Chim. Acta* **1988**, *144*, 81−87.

(14) The opposite trend was observed with the related sulfur-bridged ligand $\{OSO^{Me}\}^{2-}$; that is, alcohol elimination reactions of $\{OSO^{Me}\}H_2$ were selective with $Zr(OtBu)_4$ but not with $Ti(OiPr)_4$; see ref 9.

Scheme 1

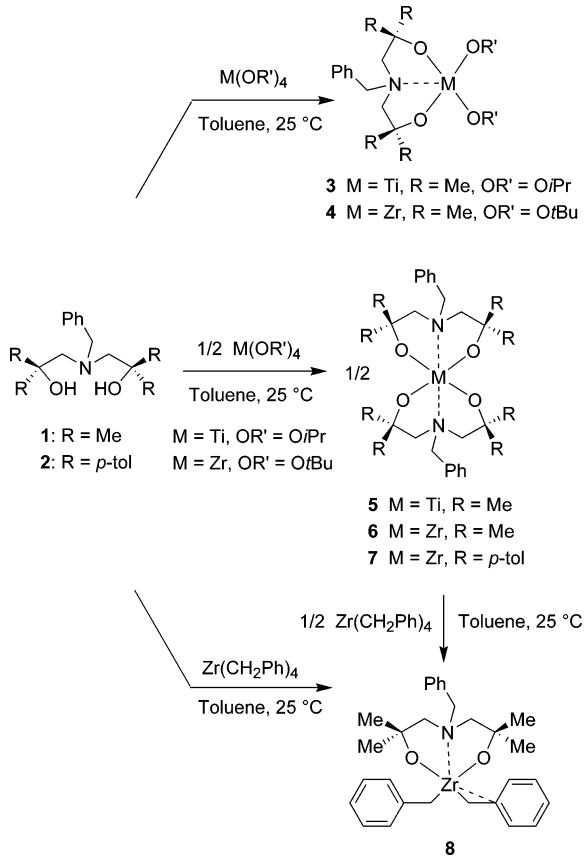

Scheme 2

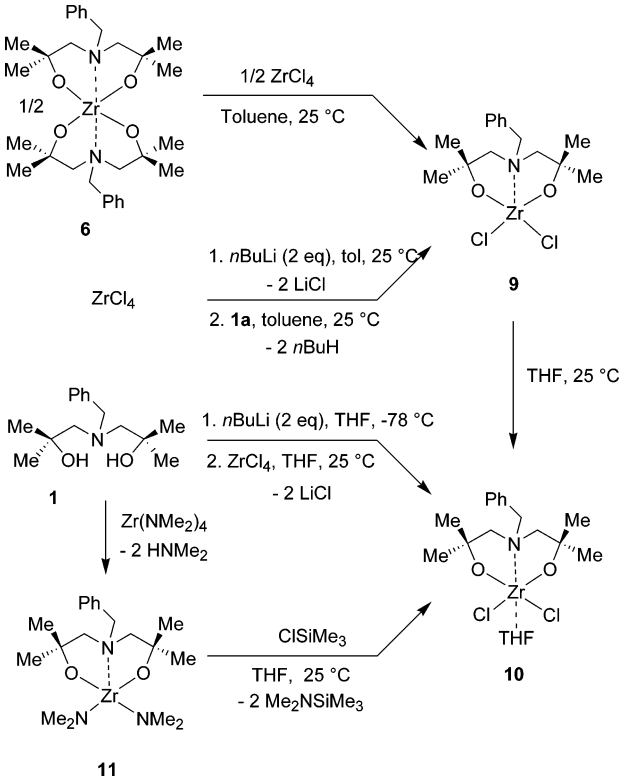

Two $\{ONO^{Me}\}ZrCl_2(THF)_n$ complexes with a variable number of THF ligands (n = 0, 1) were prepared as shown in Scheme 2. Comproportionation of bis-ligand complex **6** with $ZrCl_4$ in toluene gave the THF-free complex $\{ONO^{Me}\}ZrCl_2$ (**9**) in virtually quantitative yield. Complex **9** was also prepared in a one-pot procedure by generating first "$Zr(n\text{Bu})_2Cl_2$" from $ZrCl_4$ and nBuLi[15] and then adding 2 equiv of **1** to perform an alkane elimination. Salt metathesis between $ZrCl_4(THF)_2$ and the in situ-generated dilithium salt of **1**, $Li_2\{ONO^{Me}\}$, proceeded readily in THF solution to give the dichloro complex with a single THF ligand $\{ONO^{Me}\}ZrCl_2(THF)$ (**10**). Alternatively, reaction of $Zr(NMe_2)_4$ with 2 equiv of **1** gave in quantitative yield the diamido complex $\{ONO^{Me}\}Zr(NMe_2)_2$ (**11**),[16] which was further converted to dichloro complex **10** upon treatment with $ClSiMe_3$ in THF solution.

THF-free dichlorotitanium complexes $\{ONO^{R}\}TiCl_2$ (**13**, R = Me; **14**, R = *p*-tol) were prepared by alcohol elimination between the corresponding diol (**1** and **2**, respectively) and $Ti(OiPr)_2Cl_2$,[10,17] in situ-generated from $TiCl_4$ and $Ti(OiPr)_4$ (eq 3).

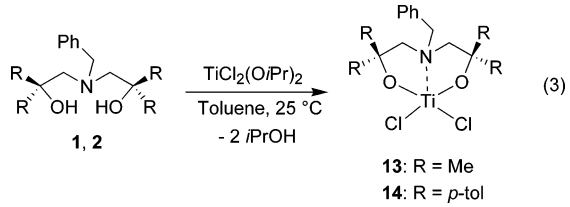

Solid-State Structures of Neutral Complexes. The solid-state structures of **3**, **6**, **8**, **12**,[16] **13**, and **14** were determined by single-crystal X-ray diffraction studies. Crystallographic data and selected bond distances and angles are listed in Tables 1−7.

The solid-state structures of **3**, **13**, and **14** are quite similar and will be discussed first (Figures 1−3). These compounds all adopt five-coordinate, distorted trigonal bipyramidal, monomeric structures in which the equatorial positions are occupied by the two oxygen atoms of the chelating dialkoxide and an additional X ligand (O*i*Pr and Cl, respectively).[18] The nitrogen atom is coordinated on an axial position. A (noncrystallographic) plane of symmetry embraces the Ti, N, and both X atoms, which confers an approximate C_s symmetry to these molecules. The Ti−O bond distances involving the chelating dialkoxide ligand in the three compounds differ within less than 0.02 Å in a given complex. In the dichloro complexes **13** and **14**, those distances are similar (1.767(2)−1.792(1) Å), indicative of a minimal steric influence of the R substituent α to O (Me vs *p*-tol), and compare well with those observed in the related complex $\{OSO^{Me}\}TiCl_2(THF)_2$ (1.761(2), 1.765(2) Å).[9] Somewhat longer Ti−O bond distances are observed in the isopropoxide complex **3** (1.842(1)−1.852(1) Å), possibly reflecting the higher electron density at the metal

(15) (a) Eisch, J. J.; Owuor, F. A.; Shi, X. *Organometallics* **1999**, *18*, 1583−1585. (b) Eisch, J. J.; Owuor, F. A.; Otieno, P. O. *Organometallics* **2001**, *20*, 4132−4134.

(16) The identity of **11** was unambiguously confirmed by elemental analysis and its reactivity (selective conversion to **10**). The ^{1}H NMR spectra of **11** in toluene-d_8 and THF-d_8 featured many unresolved resonances, indicative of the presence of several species in solution. Upon recrystallization of **11** from toluene, X-ray suitable crystals of $\{\kappa^2\text{-}ONO^{Me}\}Zr(\mu^2\text{-}NMe_2)(\mu^2,\kappa^3\text{-}\{ONO^{Me}\})Zr(\kappa^2\text{-}\{ONO^{Me}\})(NMe_2)$ (**12**), a dimeric species that results from the exchange of two NMe_2 units by a $\{ONO^{Me}\}^{2-}$ moiety, were isolated.

(17) Gothelf, K. V.; Jorgensen K. A. *J. Org. Chem.* **1994**, *59*, 5687−5691.

(18) Dihedral angles: **3**, Ti(1)−O(2)−O(8)−O(20) = 37.79°; **8**, Zr(1)−C(23)−C(24)−N(1) = 2.18°; **13**, Ti(1)−O(1)−O(2)−Cl(1) = 31.65°; **14**, Ti(1)−O(1)−O(2)−Cl(1) = 33.03°.

Table 1. Crystal Data and Structure Refinement for 3, 6, 8, 12, 13, and 14

	3	**6**·C_5H_{12}	**8**·C_6H_6	**12**	**13**·$2C_6H_6$	**14**·C_7H_8
formula	$C_{21}H_{37}NO_4Ti$	$C_{60}H_{92}N_4O_8Zr_2$	$C_{29}H_{37}NO_2Zr$	$C_{26.25}H_{42.50}N_{2.50}O_3Zr$	$C_{15}H_{23}NO_2TiCl_2$	$C_{39}H_{39}NO_2TiCl_2$
cryst size, mm	0.06 × 0.03 × 0.01	0.35 × 0.33 × 0.21	0.25 × 0.10 × 0.10	0.07 × 0.03 × 0.03	0.25 × 0.22 × 0.12	0.25 × 0.20 × 0.18
M, g·mol^{-1}	415.42	1251.96	600.92	532.35	524.36	764.62
cryst syst	orthothombic	orthorhombic	triclinic	triclinic	monoclinic	triclinic
space group	*Pbca*	*Pbca*	$P\bar{1}$	$P\bar{1}$	$P2_1/n$	$P\bar{1}$
a, Å	9.23220(10)	25.9133(2)	8.2126(15)	10.2018(3)	8.9747(2)	11.6927(2)
b, Å	16.1665(2)	21.78440(10)	11.844(2)	15.2094(4)	17.5058(4)	12.8447(3)
c, Å	30(0860(5)	23.7752(2)	15.873(3)	19.0889(5)	17.6712(4)	13.5239(4)
α, deg	90.00	90.00	88.381(3)	75.4540(10)	90.00	93.4990(10)
β, deg	90.00	90.00	82.016(3)	76.6110(10)	95.0630(10)	103.2660(10)
γ, deg	90.00	90.00	87.221(3)	80.5690(10)	90.00	97.669(2)
V, Å^3	1526.9(5)	13421.24(17)	1526.9(5)	2771.41(13)	2765.48(11)	1950.37(8)
Z	2	8	2	4	4	2
D_{calc}, Mg/m^3	1.307	1.239	1.307	1.276	1.259	1.302
T, K	100(2)	120(1)	100(2)	100	150(1)	120(1)
θ range, deg	1.72−28.32	2.06−27.49	1.72−28.32	3.11	1.64−27.50	2.13−27.51
μ, mm^{-1}	0.391	0.363	0.391	31.01	0.525	0.396
no. of measd reflns	18097	210699	18097	48557	37757	25631
no. of indep reflns	7157	15400	7601	17693	6356	8976
no. of reflns $I>2\sigma(I)$	6431	12611	6431	14018	4289	7155
no. of params	356	687	356	582	353	470
goodness of fit	1.034	1.125	1.034	1.089	1.029	1.027
R {$I > 2\sigma(I)$}	0.0325	0.0520	0.0325	0.0585	0.0500	0.0481
wR_2	0.0756	0.1248	0.0756	0.1430	0.1345	0.1230
lgst diff, e·Å^{-3}	0.398	1.192	0.609	2.427	0.575	0.499

Table 2. Selected Bond Lengths (Å) and Angles (deg) for 3

N(5)−Ti(1)	2.4473(12)	C(22)−O(20)-Ti(1)	135.99(10)
O(8)−Ti(1)	1.8518(11)	O(10)−Ti(1)-N(5)	170.35(5)
O(2)−Ti(1)	1.8418(11)	O(8)−Ti(1)-N(5)	75.77(4)
O(10)−Ti(1)	1.7856(11)	O(2)−Ti(1)-N(5)	76.14(4)
O(20)−Ti(1)	1.8102(11)	O(20)−Ti(1)−N(5)	86.47(4)
C(7)−O(8)−Ti(1)	126.59(9)	O(10)−Ti(1)−O(20)	103.16(5)
C(3)−O(2)−Ti(1)	127.11(9)	O(2)−Ti(1)−O(10)	100.35(5)
C(12b)−O(10)−Ti(1)	159.6(3)	O(8)−Ti(1)−O(10)	99.45(5)

Table 3. Selected Bond Lengths (Å) and Angles (deg) for 13·$2C_6H_6$

N(1)−Ti(1)	2.3743(17)	Cl(2)−Ti(1)−N(1)	172.26(7)
O(1)−Ti(1)	1.7827(17)	O(1)−Ti(1)-O(2)	118.83(9)
O(2)−Ti(1)	1.7670(18)	O(1)−Ti(1)−Cl(1)	116.63(6)
Cl(1)−Ti(1)	2.2610(8)	O(2)−Ti(1)−Cl(1)	116.78(7)
Cl(2)−Ti(1)	2.2852(7)	O(2)−Ti(1)−Cl(2)	100.41(6)
C(1)−O(1)−Ti(1)	131.64(14)	O(1)−Ti(1)−N(1)	76.26(7)
C(5)−O(2)−Ti(1)	133.13(15)	O(2)−Ti(1)−N(1)	75.73(7)

Table 4. Selected Bond Lengths (Å) and Angles (deg) for 14·C_7H_8

N(1)−Ti(1)	2.3377(17)	Cl(2)−Ti(1)−N(1)	164.52(5)
O(1)−Ti(1)	1.7917(15)	O(2)−Ti(1)−O(1)	126.27(7)
O(2)−Ti(1)	1.7924(14)	O(1)−Ti(1)−Cl(1)	113.27(5)
Cl(1)−Ti(1)	2.2496(6)	O(2)−Ti(1)−Cl(1)	112.78(5)
Cl(2)−Ti(1)	2.2684(6)	O(2)−Ti(1)−Cl(2)	97.73(5)
C(1)−O(1)−Ti(1)	131.17(12)	O(1)−Ti(1)−N(1)	75.54(6)
C(4)−O(2)−Ti(1)	131.93(12)	O(2)−Ti(1)−N(1)	75.52(6)

center. The Ti−O−C angles in **3** (126.59(9)°, 127.11(9)°), **13** (131.6(1)°, 133.1(1)°), and **14** (131.2(1)°, 131.9(1)°) are bent to the same extent as in the diamino-dialkoxide-Ti complex {{−$CH_2N(Me)CH_2C(CF_3)_2O$}$_2$}$TiCl_2$ (129.8(1)°, 129.4(1)°).[8] It is reasonable to describe the oxygens in complexes **3**, **13**, and **14** as sp^2-hybridized and to regard the alkoxides as four-electron (*σ*, *π*) donors; however, because of the more acute M−O−C angles, the oxygens in these complexes are less donor than in Berg's six-membered-ring amino-dialkoxide species {N{CH_2-$CH_2C(O)Me_2$}$_2$}ZrX_2, resulting in higher electron-deficiency at the metal center. The five-membered chelate rings in **3**, **13**, and **14** are rather flat and appear not to be significantly strained. Due to the *trans* influence of the O*i*Pr ligand, the Ti−N bond distance (2.447(1) Å) in **3** is longer than in chloro complexes **13** (2.374(2) Å) and **14** (2.338(2) Å).

Table 5. Selected Bond Lengths (Å) and Angles (deg) for 8·C_6H_6

N(1)−Zr(1)	2.4056(15)	C(24)−C(23)−Zr(1)	83.04(11)
O(1)−Zr(1)	1.9667(12)	C(17)−C(16)−Zr(1)	101.81(11)
O(2)−Zr(1)	1.9625(12)	O(1)−Zr(1)−O(2)	144.96(5)
C(16)−Zr(1)	2.3008(18)	O(1)−Zr(1)−C(16)	101.26(6)
C(17)−Zr(1)	2.977(18)	O(1)−Zr(1)−C(24)	103.04(6)
C(23)−Zr(1)	2.2917(18)	N(1)−Zr(1)−C(24)	143.94(6)
C(24)−Zr(1)	2.561(18)	N(1)−Zr(1)−C(16)	123.54(6)
C(1)−O(1)−Zr(1)	129.47(11)	N(1)−Zr(1)−O(1)	72.36(5)
C(6)−O(2)−Zr(1)	130.23(10)	N(1)−Zr(1)−O(2)	72.73(5)

Table 6. Selected Bond Lengths (Å) and Angles (deg) for 6·C_5H_{12}

O(1)−Zr(1)	1.957(2)	C(1)−O(1)−Zr(1)	151.37(19)
O(2)−Zr(1)	1.963(2)	C(5)−O(2)−Zr(1)	151.6(2)
O(3)−Zr(1)	2.223(2)	C(16)−O(3)−Zr(1)	140.18(17)
O(3)−Zr(2)	2.2159(19)	C(16)−O(3)−Zr(2)	119.19(16)
O(4)−Zr(1)	2.2870(19)	C(20)−O(4)−Zr(1)	131.49(16)
O(4)−Zr(2)	2.198(2)	C(20)−O(4)−Zr(2)	116.65(16)
O(5)−Zr(2)	1.941(2)	C(35)−O(5)−Zr(2)	163.5(2)
O(6)−Zr(2)	1.951(2)	C(31)−O(6)−Zr(2)	160.51(19)
O(7)−Zr(1)	2.3454(19)	C(50)−O(7)−Zr(1)	128.45(16)
O(7)−Zr(2)	2.054(2)	C(50)−O(7)−Zr(2)	134.11(17)
O(8)−Zr(1)	1.949(2)	C(46)−O(8)−Zr(1)	157.90(19)
Zr(1)−Zr(2)	3.2342(4)	O(1)−Zr(1)−O(2)	97.89(9)
N(2)−Zr(2)	2.395(2)	O(1)−Zr(1)−O(8)	101.58(9)
O(2)−Zr(1)−O(4)	159.95(8)	O(2)−Zr(1)−O(7)	93.67(8)
O(1)−Zr(1)−O(7)	164.60(8)	O(2)−Zr(1)−O(8)	99.58(9)
O(3)−Zr(1)−O(8)	154.18(8)	O(3)−Zr(2)−O(4)	73.53(7)
O(3)−Zr(2)−O(5)	198.42(8)	O(3)−Zr(2)−O(6)	94.22(8)
O(4)−Zr(2)−O(6)	165.16(8)	O(3)−Zr(2)−N(2)	70.00(8)
O(7)−Zr(2)−N(2)	139.82(8)		

The solid-state structure of the dibenzyl complex **8** (Figure 4) follows the gross features of the compounds previously discussed. The coordination of the {ONO^{Me}}$^{2-}$ ligand is meridional with the two oxygens occupying the axial sites; the O−Zr−O angle (144.96(5)°) is, however, significantly smaller than 180°.[18] The Zr−O distances (1.967(1), 1.963(1) Å) are ca. 0.15−0.20 Å longer than the corresponding Ti−O bonds, reflecting the ca. 15% difference in the metal ionic radii,[19] and fall in the range

Table 7. Selected Bond Lengths (Å) and Angles (deg) for 12

O(2a)−Zr(1a)	1.931(2)	C(3a)−O(2a)−Zr(1a)	164.4(2)
O(8a)−Zr(1a)	1.990(2)	C(7a)−O(8a)−Zr(1a)	139.0(2)
O(2c)−Zr(1a)	2.273(2)	C(3c)−O(2c)−Zr(1a)	131.82(17)
O(8c)−Zr(1a)	2.263(2)	C(7c)−O(8c)−Zr(1a)	139.62(17)
O(2b)−Zr(1b)	1.950(2)	C(3b)−O(2b)−Zr(1b)	159.63(19)
O(8b)−Zr(1b)	1.948(2)	C(7b)−O(8b)−Zr(1b)	162.3(2)
O(2c)−Zr(1b)	2.224(2)	C(3c)−O(2c)−Zr(1b)	114.74(17)
O(8c)−Zr(1b)	2.196(2)	C(7c)−O(8c)−Zr(1b)	118.97(17)
N(22)−Zr(1a)	2.094(3)	O(8b)−Zr(1b)−O(8c)	169.64(8)
N(25)−Zr(1a)	2.434(3)	O(2b)−Zr(1b)−O(2c)	166.55(8)
N(25)−Zr(1b)	2.157(3)	N(25)−Zr(1b)−O(5c)	141.87(9)
N(5c)−Zr(1b)	2.388(2)	O(2a)−Zr(1a)−O(8a)	96.47(9)
Zr(1a)−Zr(ab)	3.2502(4)	O(2a)−Zr(1a)−N(22)	95.40(10)
N(25)−Zr(1a)−O(8a)	163.20(9)	O(2a)−Zr(1a)−N(25)	93.44(9)
N(22)−Zr(1a)−O(8c)	158.07(10)	O(2a)−Zr(1a)−O(8c)	96.78(9)
N(2a)−Zr(1a)−O(2c)	163.93(9)	O(8a)−Zr(1a)−O(8c)	95.36(8)

(ca. 1.95−2.08 Å) observed for alkoxy-Zr complexes.[5−7,9,20] The Zr−N distance of 2.406(2) Å is similar to that of 2.419(12) Å found in the parent complex Zr{N{CH_2-$CH_2C(O)Me_2$}$_2${((*S*)-2-$C_6H_4C(H)Me$}}{CH_2Ph}.[6] As in the latter complex, one benzyl group in **8** is η^2-coordinated, as evident from the acute Zr(1)−C(23)−C(24) angle of 83.0(1)° and the short Zr(1)−C(24) contact of 2.56(2) Å.[7,21] We assume that η^2-coordination of a benzyl group in **8** reflects the electron-deficiency of this compound (formally 14-e), as supported by acute Zr−O−C angles (129.5(1)°, 130.2(1)°).[5]

The bis-ligand complex **6** adopts a dimeric structure in which both zirconium atoms are in a highly distorted octahedral coordination geometry (Figure 5). Two $\{ONO^{Me}\}^{2-}$ ligands are in a terminal mode, while two others bridge the zirconiums, with regular Zr−O bond distances and Zr−O−C angles.[22] Only one out of the four

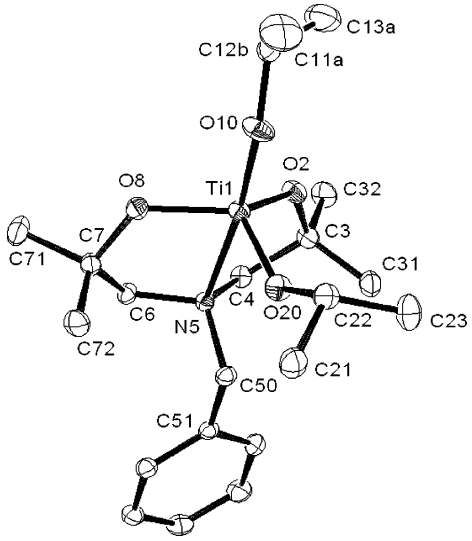

Figure 1. ORTEP view of $\{ONO^{Me}\}Ti(OiPr)_2$ (**3**). Ellipsoids are drawn at the 30% probability level; all hydrogen atoms have been omitted for clarity.

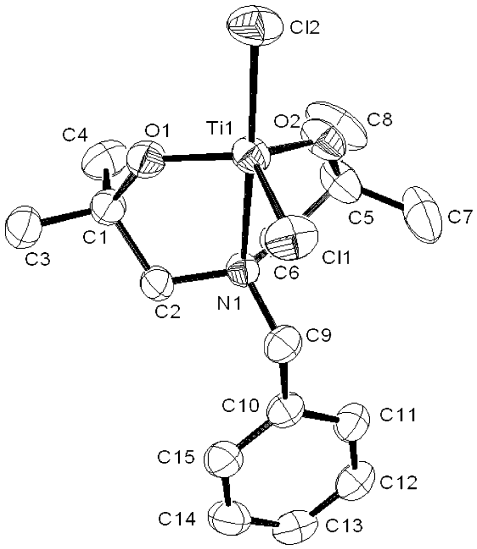

Figure 2. ORTEP view of $\{ONO^{Me}\}TiCl_2$ (**13**). Ellipsoids are drawn at the 50% probability level; all hydrogen atoms have been omitted for clarity.

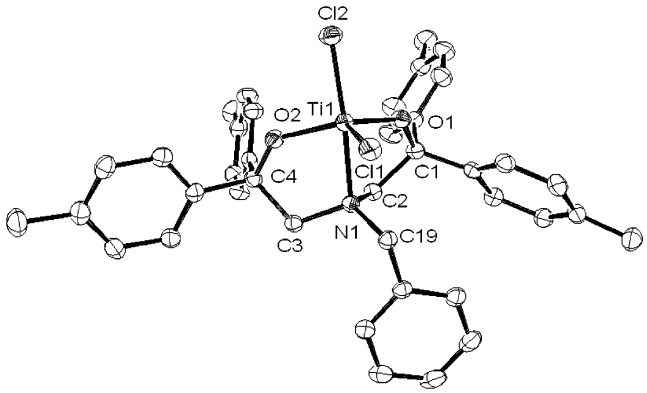

Figure 3. ORTEP structure of $\{ONO^{tol}\}TiCl_2$ (**14**). Ellipsoids are drawn at the 30% probability level; all hydrogen atoms have been omitted for clarity.

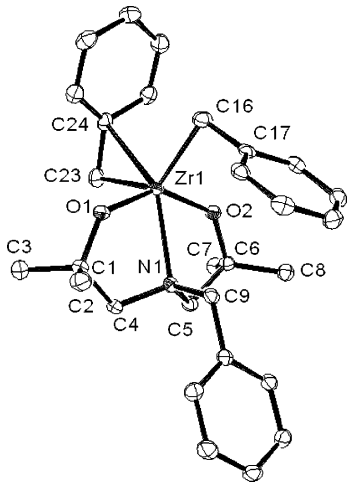

Figure 4. ORTEP view of $\{ONO^{Me}\}Zr(CH_2Ph)_2$ (**8**). Ellipsoids are drawn at the 30% probability level; all hydrogen atoms have been omitted for clarity.

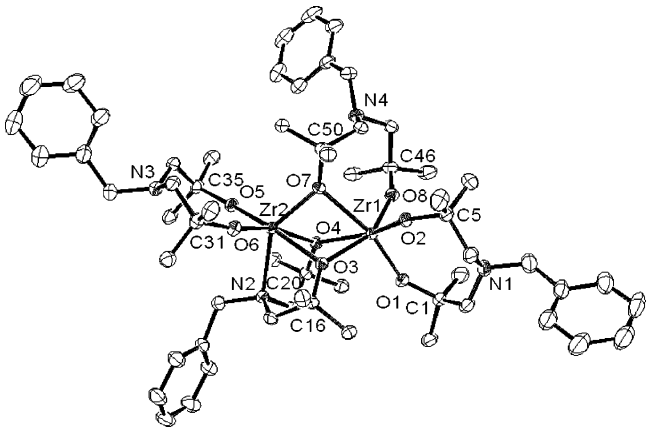

Figure 5. ORTEP view of $\{ONO^{Me}\}_2Zr$ (**6**). Ellipsoids are drawn at the 30% probability level; all hydrogen atoms have been omitted for clarity.

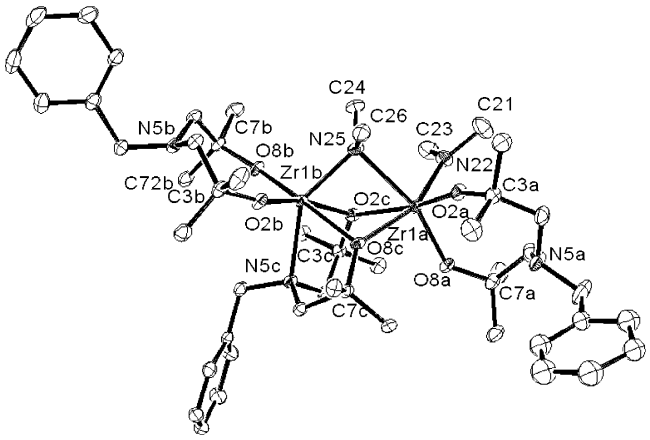

Figure 6. ORTEP view of **12**. Ellipsoids are drawn at the 30% probability level; all hydrogen atoms have been omitted for clarity.

nitrogens is coordinated to Zr, and the overall molecule is dissymmetric. The dinuclear structure of **6** contrasts with the mononuclear structures observed for the six-membered bis(amino-dialkoxide) complex $Zr\{MeN\{CH_2CH_2C(O)Ph_2\}_2\}_2$, in which both nitrogen atoms are coordinated to the metal center,[5b] and the five-membered sulfur-birdged complex $Ti\{OSO^{Me}\}_2$, which has a tetrahedral coordination.[9] We assume that, in these cases, larger substituents at the α-positions (R = Ph vs Me) and a smaller metal center (Ti vs Zr), respectively, prevent dimerization. Unfortunately, no suitable X-ray crystal of $\{ONO^{tol}\}_2Zr$ (**7**) could be obtained to assess this hypothesis.

Complex **12**, isolated during the synthesis of amido complex **11**,[16] exhibits a dimeric structure very similar to that of **6** (Figure 6). Formally, the two structures are obtained by replacing the $\{ONO^{Me}\}^{2-}$ ligand in a mixed terminal−bridging mode by two NMe_2 groups playing the same role.

The structures of **6** and **12** are similar to that observed for $\{\{OSO^{Me}\}Zr(OtBu)_2\}_2$, i.e., $(OtBu)_2Zr(\mu^2\text{-}OtBu)(\mu^2,\kappa^3\text{-}\{OSO^{Me}\})Zr(\kappa^2\text{-}\{OSO^{Me}\})(OtBu)$;[9] these structures all display a bridging $\{OZO^{Me}\}^{2-}$ ligand with a singly coordinated Z atom (Zr(2)−N(2) = 2.395(2) Å in **6**; Zr(1b)−N(5c) = 2.388(2) Å in **12**; Zr−S = 2.768(1) Å[9]).

Solution Structure and Dynamics of Neutral Complexes. The solution structures and dynamic behaviors of the prepared complexes have been investigated by variable-temperature NMR spectroscopy. Assignment of ^1H and ^{13}C resonances was made from 2D COSY, HMQC, and HMBC experiments. NMR studies were performed in toluene or benzene solvent to avoid the formation of solvent adducts.

The 261 K ^1H NMR spectrum of $\{ONO^{Me}\}TiCl_2$ (**13**) in toluene-d_8 features sharp signals (Figure 7). Key resonances include one singlet for the NCH_2Ph group, two AB doublets for the NC*HH* groups, and two singlets for the CMe_2 groups. The 243 K ^{13}C NMR spectrum of **13** contains one set of benzyl resonances, one NCH_2 resonance, and one methyl resonance. These data are consistent with overall C_s symmetry. Coordination of the N atom to Ti in **13** is most likely, as expected from the metal center's electron deficiency and as observed in the solid-state structure, but the NMR data give no definitive evidence for it.[23]

As shown in Figure 7, raising the temperature results in broadening and coalescence of the NC*HH* resonances (T_{coal} = ca. 300 K) and the methyl resonances (T_{coal} = 285 K), and at 320 K singlets are observed for those groups. These data establish that **13** undergoes an exchange process, as shown in eq 4. Line-shape analysis confirmed that both the NCH_2CMe_2 hydrogens and the CMe_2 hydrogens exchange at the same (or at least quite similar) rates (Figure 7), as expected for the fluxional process in eq 4. The activation parameters for this fluxional behavior ($\Delta H^{\ddagger} = 17.4 \pm 0.5$ kcal·mol^{-1}; $\Delta S^{\ddagger} = 11.4 \pm 2$ cal·mol^{-1}·K^{-1}) were derived from an Eyring analysis (Figure 8).[24]

A similar fluxional behavior was observed for $\{ONO^{Me}\}Ti(OiPr)_2$ (**3**). The 252 K ^1H NMR spectrum of **3** features the same pattern of resonances for the $\{ONO^{Me}\}^{2-}$ ligand as that observed for **13**, together with

(19) Effective ionic radii for six-coordinate metal centers: Ti^{4+}, 0.605 Å; Zr^{4+}, 0.72 Å. Shannon, R. D. *Acta Crystallogr., Sect. A* **1976**, *A32*, 751−767.

(20) (a) Howard, W. A.; Trnka, T. M.; Parkin, G. *Inorg. Chem.* **1995**, *34*, 5900−5909. (b) Stephan, D. W. *Organometallics* **1990**, *9*, 2718−2723. (c) Tsukahara, T.; Swenson, D. C.; Jordan, R. F. *Organometallics* **1997**, *16*, 3303−3313.

(21) (a) Latesky, S. L.; McMullen, A. K.; Niccolai, G. P.; Rothwell, I. P.; Huffman, J. C. *Organometallics* **1985**, *4*, 902−908. (b) Jordan, R. F.; Lapointe, R. E.; Bajgur, C. S.; Echols, S. F.; Willett, R. *J. Am. Chem. Soc.* **1987**, *109*, 4111−4113. (c) Bochmann, M.; Lancaster, S. J.; Hursthouse, M. B.; Malik, K. M. A. *Organometallics* **1994**, *13*, 2235−2243.

(22) For examples of dimeric Zr alkoxides, see: (a) Evans, W. J.; Ansari M. A.; Ziller J. W. *Inorg. Chem.* **1999**, *38*, 1160−1164. (b) Fleeting, K. A.; O'Brien P.; Jones, A. C.; Otway, D. J.; White, A. J. P.; William, D. J. *J. Chem. Soc., Dalton Trans.* **1999**, 2853−2859. (c) Vaartstra, B. A.; Huffman, J. C.; Gradeff, P. S.; Hubert-Pfalzgraf, L.-G.; Daran, J.-C.; Parraud, S.; Yunlu, K.; Caulton, K. G. *Inorg. Chem.* **1990**, *29*, 3126−3131.

(23) No clear trend was observed in the ^1H and ^{13}C chemical shifts of the NCH_2CR_2 and NCH_2Ph units in complexes prepared in this study that could be related to coordination of N to the metal center.

(24) (a) These values correspond well with the free energies of activation determined experimentally from the coalescence temperatures for both the NCH_2CMe_2 (T_c = 300 K; $\Delta G_{coal}^{\ddagger}$ = 13.9(3) kcal·mol^{-1}; $\Delta G_{calc}^{\ddagger}$ = 14.0 kcal·mol^{-1}) and CMe_2 hydrogens (T_c = 285 K; $\Delta G_{coal}^{\ddagger}$ = 14.3(3) kcal·mol^{-1}; $\Delta G_{calc}^{\ddagger}$ = 14.2 kcal·mol^{-1}). Exchange barriers $\Delta G^{\ddagger}$ were determined from the coalesence of the NCH_2 AB patterns using the following equations for an equally populated, two-site exchange: $\Delta G^{\ddagger} = 4.576T_c\{10.319 + \log(T_c/k_c)\}$ (kcal·mol^{-1}), where T_c is the coalesence temperature and k_c is the exchange rate constant at coalesence, which is given by $k_c = \pi\{(\Delta\nu_{AB}^2 + 6J_{AB}^2\}^{1/2}/2^{1/2}$. The errors on $\Delta G_{coal}^{\ddagger}$ were estimated assuming ±2% uncertainty in the chemical shifts and coalescence temperature.[b−d] (b) Alexander, S. *J. Chem. Phys.* **1962**, *37*, 967−974. (c) Kurland, R. J.; Rubin, M. B.; Wise, W. B. *J. Chem. Phys.* **1964**, *40*, 2426−2427. (d) Kost, D.; Zeichner, A. *Tetrahedron Lett.* **1974**, 4533−4536.

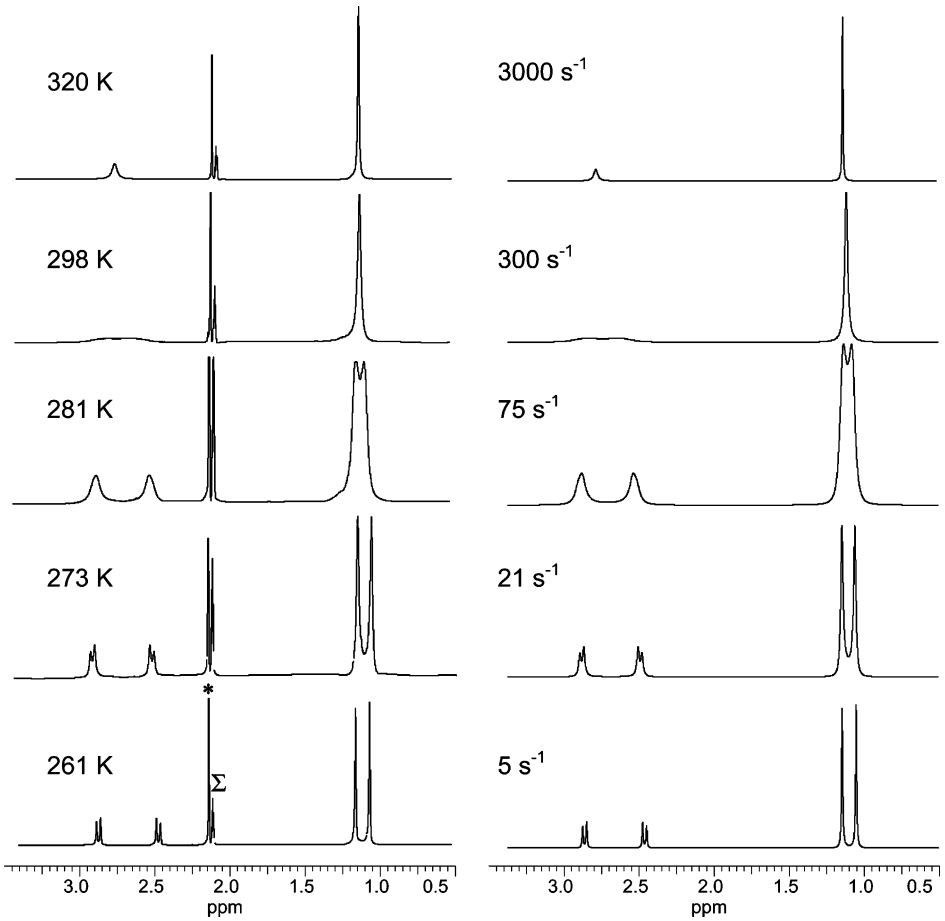

Figure 7. Experimental (left) and simulated (right) variable-temperature ^{1}H NMR spectra of {ONO^{Me}}TiCl$_2$ (**13**) showing the NCH_2CMe$_2$ (δ 2.80 and 2.50) and CMe_2 (δ 1.20 and 1.05) resonances (toluene-d_8, 400 MHz). The vertical expansion is different in each case for clarity. Best-fit first-order rate constants (k) are shown with the simulated spectra. The markers * and Σ denote resonances for PhCH_3 and PhCHD$_2$, respectively.

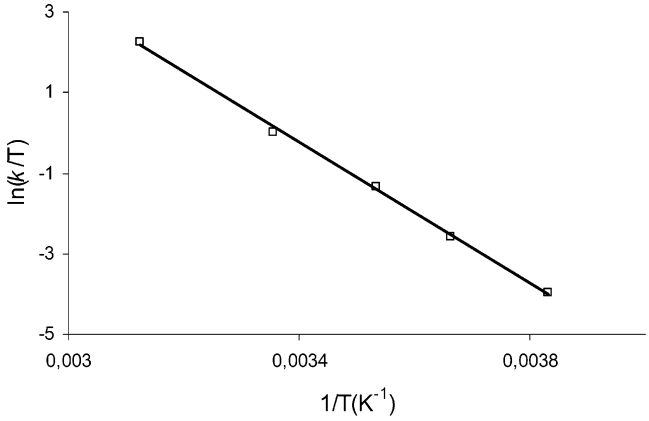

Figure 8. Eyring plot for {ONO^{Me}}TiCl$_2$ (**13**) (toluene-d_8 solvent).

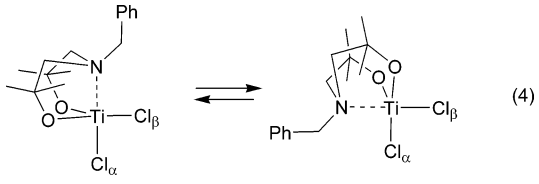

(4)

two doublets for inequivalent CH_3 in the OiPr groups. At 320 K, three sharp singlets are observed for the CH_3, NCH_2CMe$_2$, and NCH_2Ph hydrogens of the ligand, and the OCH(CH_3)$_2$ hydrogens appear as a sharp doublet. The free energy of activation determined from the coalescence temperature for the NCH_2CMe$_2$ hydrogens in **3** (T_c = 285 K; $\Delta G_{coal}^{\ddagger}$ = 13.0 ± 0.3 kcal·mol^{-1}) is slightly lower than that obtained for **13** ($\Delta G^{\ddagger}$ (285 K) = 14.3 kcal·mol^{-1}).[24] The similarity of these data indicates limited influence of the X (Cl, OiPr) ligands on the overall dynamics of {ONO^{Me}}TiX$_2$ complexes **3** and **13**.

The 298 K ^{1}H NMR spectrum of the dichlorotitanium complex {ONO^{tol}}TiCl$_2$ (**14**), which bears p-tolyl substituents at the α positions in place of the methyl groups in **13**, displays the same characteristic sharp resonances as those observed for **13** at low temperature. The AB system for the inequivalent NCHHC(p-tol)$_2$ hydrogens, a singlet for the NCH_2Ph hydrogens, and two singlets for the p-C$_6$H$_4$$Me$ groups indicate also a C_s-symmetric structure with a mirror plane including the Ti, N, and both Cl atoms. Upon heating, the Me p-tol resonances coalesce first (T_{coal} = 345 K; $\Delta G_{coal}^{\ddagger}$ = 17.7 ± 0.3 kcal·mol^{-1}) and then those of the NCHHC(p-tol)$_2$ (T_{coal} = 357 K; $\Delta G_{coal}^{\ddagger}$ = 17.6 ± 0.3 kcal·mol^{-1}) (see Supporting Information).

The dibenzyl complex {ONO^{Me}}Zr(CH$_2$Ph)$_2$ (**8**) features dynamics in toluene solution similar to those of **3**, **13**, and **14** (Figure 9). The room-temperature ^{1}H NMR spectrum of **8** is in the slow exchange regime, and freezing/resolution is achieved at 250 K. In addition to the sharp AB doublets (NCHHCMe$_2$), the two singlets (NCH$_2$CMe_2), and the singlet (NCH_2Ph, δ 3.56, not shown in Figure 9) observed for **13**, the low-temperature

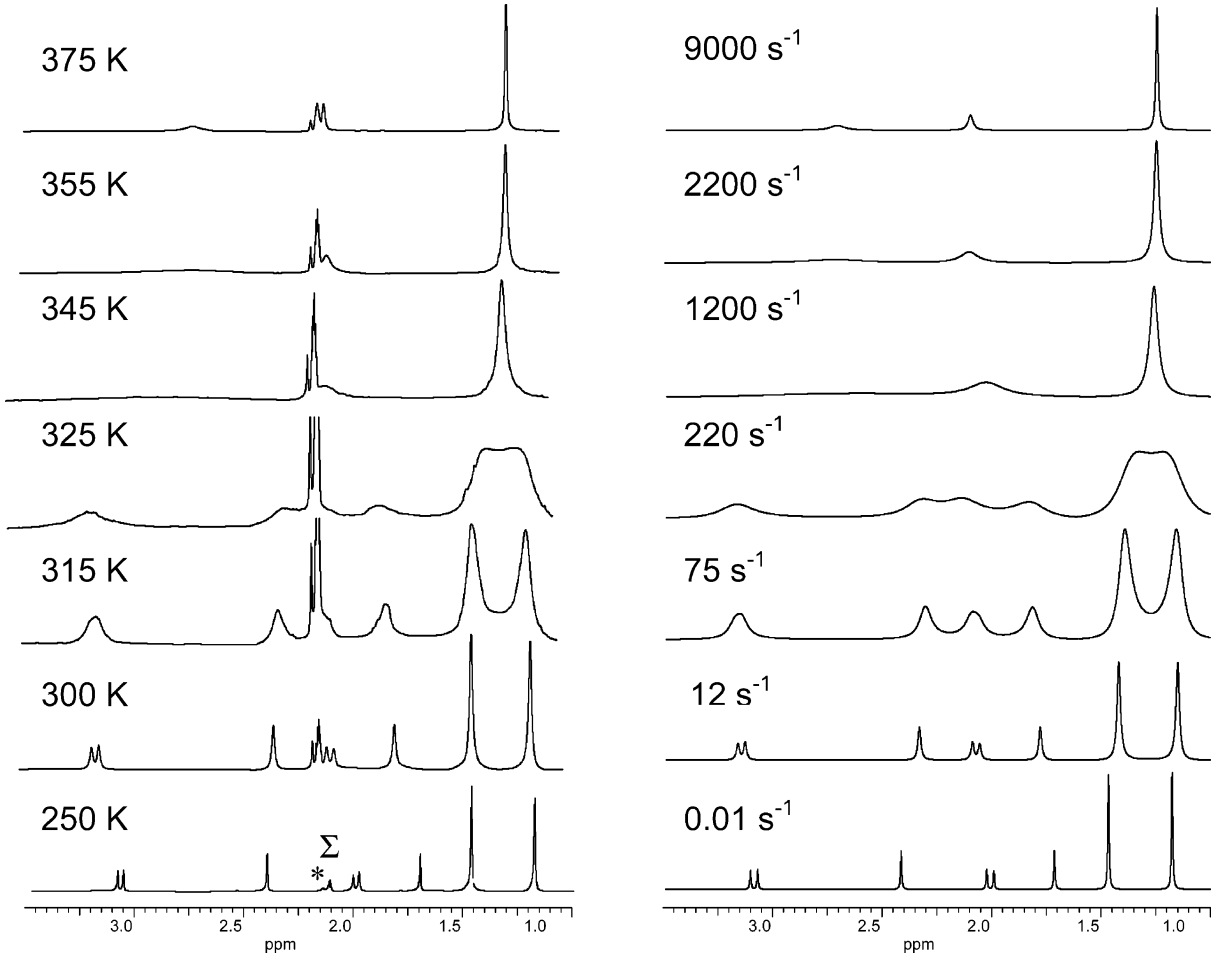

Figure 9. Experimental (left) and simulated (right) variable-temperature ^{1}H NMR spectra of {ONO^{Me}}Zr(CH$_2$Ph)$_2$ (**8**) showing the NC*H*$_2$CMe$_2$ (δ 3.15 and 2.00), ZrC*H*$_2$Ph (δ 2.35 and 1.75), and C*Me*$_2$ (δ 1.45 and 1.15) resonances (toluene-d_8, 400 MHz). The vertical expansion is different in each case for clarity. Best-fit first-order rate constants (k) are shown with the simulated spectra. The markers * and Σ denote resonances for PhC*H*$_3$ and PhC*H*D$_2$, respectively.

spectrum of **8** displays two singlets for the ZrC*HH*Ph hydrogens. The observation of two C$_{ipso}$ signals for the benzyl rings in the ^{13}C spectrum, with one high-field and one low-field resonance (δ 147.3 and 141.4), is diagnostic for the presence of one η^2-benzyl group and one normal η^1-benzyl group,[21] as observed in the solid state. Also, two benzylic *C*H$_2$ ^{13}C signals (δ 54.9 and 53.6) are observed. Upon warming, the ^{1}H resonance systems (except the singlet for NC*H*$_2$Ph) coalesce and, at 375 K, a total of four singlets (some still broadened) are observed. These data establish that **8** undergoes exchange of the η^2/η^1-benzyl ligands, as shown in eq 5. A line shape analysis (Figure 9) combined with an Eyring analysis (Figure 10) confirmed that the NC*H*$_2$-CMe$_2$, ZrC*H*$_2$Ph, and C*Me*$_2$ spin systems exchange at the same (or at least quite similar) rate, as expected for the fluxional process in eq 5, and gave the corresponding activation parameters ($\Delta H^{\ddagger}$ = 20.0 ± 0.5 kcal·mol^{-1}; $\Delta S^{\ddagger}$ = 13.1 ± 2 cal·mol^{-1}·K^{-1}).[25]

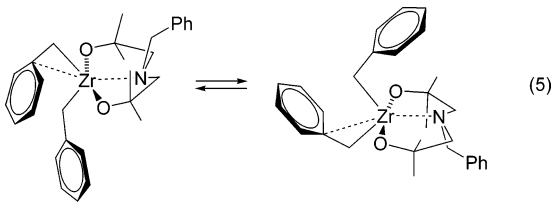

(5)

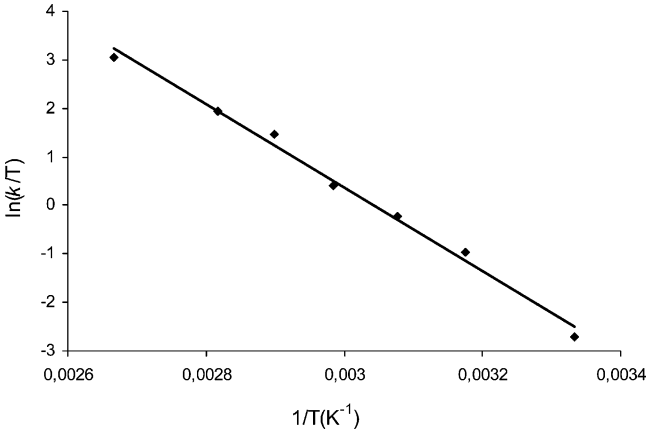

Figure 10. Eyring plot for {ONO^{Me}}Zr(CH$_2$Ph)$_2$ (**8**) (toluene-d_8 solvent).

The positive values for the entropy of activation associated with the dynamic processes for **8** and **13** ($\Delta S^{\ddagger}$ = 13.1 and 11.4 ± 2 cal·mol^{-1}·K^{-1}, respectively) are consistent with the proposed dissociative processes

(25) These values correspond well with the free energies of activation determined experimentally from the coalescence temperature for the NC*H*$_2$CMe$_2$ (T_c = 345 K; $\Delta G_{coal}^{\ddagger}$ = 15.6(3) kcal·mol^{-1}; $\Delta G_{calc}^{\ddagger}$ = 15.5 kcal·mol^{-1}), ZrCH$_2$Ph (T_c = 335 K; $\Delta G_{coal}^{\ddagger}$ = 15.7(3) kcal·mol^{-1}; $\Delta G_{calc}^{\ddagger}$ = 15.6 kcal·mol^{-1}), and C*Me*$_2$ hydrogens (T_c = 330 K; $\Delta G_{coal}^{\ddagger}$ = 15.7(3) kcal·mol^{-1}; $\Delta G_{calc}^{\ddagger}$ = 15.7 kcal·mol^{-1}). See ref 24 for calculation details.

outlined in eqs 4 and 5.[26] These processes imply dissociation of nitrogen, inversion of configuration at nitrogen, and amine re-coordination. A similar process has been proposed to account for the fluxional behavior of related zirconium bis(amino-dialkoxide)[5] and amino-diamido[27] complexes. The observation of a higher free energy exchange barrier in the bis-ligand complexes Zr{MeN{$CH_2CH_2C(O)R_2$}$_2$}$_2$ bearing phenyl substituents (R = Ph, $\Delta G^{\ddagger} \gg 15.9$ kcal·mol^{-1}) as compared to methyl-substituted systems (R = Me, $\Delta G^{\ddagger} = 15.9$ kcal·mol^{-1}) has led Berg to propose that inversion at nitrogen is more energy demanding than amine dissociation;[6] indeed, amine dissociation should be logically favored with bulkier R substituents. This hypothesis, proposed on systems where complicated processes can take place due to the presence of two amino-dialkoxide ligands on the metal center, is confirmed by our results with mono-ligand complexes. Both **8** and **13**, which have methyl substituents α to the alkoxides, show similar enthalpies of activation ($\Delta H^{\ddagger} = 20.0$ and 17.4 ± 0.5 kcal·mol^{-1}, respectively), while the exchange process for complex **14**, which has *p*-tolyl substituents at the α positions, requires more energy ($\Delta G^{\ddagger}_{\mathrm{coal}(357\ \mathrm{K})} = 17.6 \pm 0.3$ kcal·mol^{-1} for **14**, vs 15.3 and 13.3 ± 0.3 kcal·mol^{-1} for **8** and **13**, respectively).

The ^{1}H and ^{13}C NMR data for the bis-ligand complexes {ONO^R}$_2$M (**5**−**7**) in toluene solution are consistent with mononuclear structures and feature dynamic behaviors similar to those observed for the related six-membered-ring species Zr{RN{$CH_2CH_2C(O)R'_2$}$_2$}$_2$ described by Berg and co-workers.[5] The high-temperature (300−360 K) ^{1}H NMR spectra, in the fast exchange regime, all feature sharp singlets for the NCH_2CR_2, NCH_2Ph, CMe_2, and *p*-MeC$_6$H$_4$ hydrogens. In the slow exchange regime, i.e., below 250 K for **5** and **6** and below 300 K for **7**, the NCH_2Ph and NCHHCR_2 hydrogens appear as two doublets and four doublets, respectively; also, all the methyl groups are inequivalent and appear as four singlets. This fluxional behavior can also be accounted for by amine dissociation and inversion at nitrogen followed by re-coordination, a process that is hindered by bulky substituents in the case of **7**.

The NMR spectra of the dichloro complexes {ONO^{Me}}-$ZrCl_2(THF)_n$ **9** and **10** are more complicated and indicate the coexistence of several isomers and/or species in solution. The room-temperature ^{1}H NMR spectrum of the THF-free complex **9** in toluene-d_8 features several series of resonances, of which two account for more than 80% of the total. The simplest series (**9a**) contains one singlet for the NCH_2CMe_2 hydrogens and two sets of overlapping doublets for the NCH_2CMe_2 and NCH_2Ph hydrogens, suggesting a mononuclear species of high symmetry (on the NMR time scale) (e.g., **A** or **B**, Figure 11). The second series (**9b**) features four doublets for the NCHHCMe_2, four singlets for the NCH_2CMe_2, and two doublets for the NCHHPh hydrogens. Possible

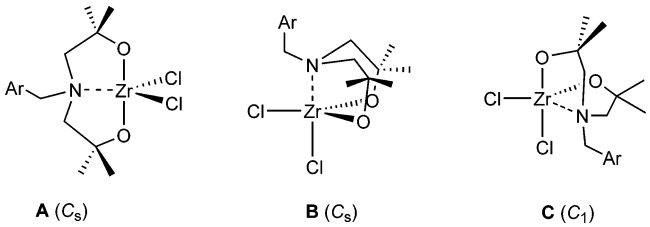

Figure 11. Plausible structures for monomeric {ONO^{Me}}-$ZrCl_2$ (**9**) (not considering isomers resulting from inversion at nitrogen)

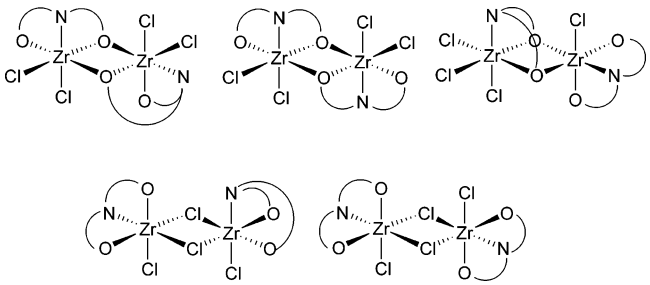

Figure 12. Schematic representations of some plausible dinuclear structures for **9**.

structures for **9b** include a C_1-symmetric monomeric species (e.g., **C**, Figure 11) or a dimeric species (Figure 12), as observed in the solid state for complexes **6** and **12** (vide supra). The **9a/9b** ratio varies from one batch to another in the range 50:50 to 40:60, but does not change with time, even after prolonged heating. The observation of several isomers or species that may have different nuclearity for **9** contrasts with the single mononuclear species observed in solution and in the solid state for the parent dichlorotitanium complexes {ONO^R}$TiCl_2$ **13** and **14.** Dimerization of **9** is plausible since Zr normally prefers a higher coordination number vs Ti.[28]

Complex **9** readily dissolves in THF to form the mono-THF adduct {ONO^{Me}}$ZrCl_2$(THF) (**10**), which is slightly soluble in benzene. Coordination of a THF ligand in **10** in the solid state was established by elemental analysis. Also, the ^{1}H and ^{13}C NMR spectrum of **10** in C_6D_6 contains resonances for a coordinated THF ligand (δ ^{1}H: 3.33, 1.71; δ ^{13}C: 70.6, 26.9), shifted upfield and downfield from free THF resonances ($\delta(C_6D_6)$ ^{1}H: 3.57, 1.40; δ ^{13}C: 67.8, 25.7).

In benzene solution, two major isomers of **10** (that account for more than 80% of the total) are also observed, one with a dissymmetric structure (**10a**) and the other with a symmetric structure (on the NMR time scale) (**10b**). The ratio **10a/10b** is ca. 70:30 and does not vary over several weeks in benzene at room temperature. The ^{1}H and ^{13}C NMR spectra of **10**-d_8 in THF-d_8 revealed the existence of three major species, **10a′**−**10c′**. The ratio **10a′/10b′/10c′** was variable according to the batch and the origin of **10** (dissolution of **9** in THF or direct synthesis via salt metathesis in THF) (see Experimental Section). However, in all cases, the kinetic mixtures slowly transformed at room temperature in THF-d_8 to yield the thermodynamic isomer, **10c′**, in more than 90% selectivity after one week. The ^{1}H and

(26) Purely dissociative mechanisms are generally characterized by $\Delta S^{\ddagger}$ values above 10 eu. See: (a) Atwood, J. D. *Inorganic and Organometallic Reaction Mechanisms*; Brooks/Cole: Monterey, CA, 1985; p 17. (b) Jordan, R. B. *Reaction Mechanisms of Inorganic and Organometallic Systems*; Oxford University: New York, 1991; pp 56−57.

(27) (a) Clark, H. C. S.; Cloke, F. G. N.; Hitchcock, P. B.; Love, J. B.; Wainwright, A. P. *J. Organomet. Chem.* **1995**, *501*, 333−340. (b) Horton, A. D.; de With, J.; van der Linden, A. J.; van de Weg, H. *Organometallics* **1996**, *15*, 2672−2674.

(28) The complex $ZrCl_2${OSO^{Me}}, which derives from the parent sulfur-bridged dialkoxide, is completely insoluble in aromatic hydrocarbons, also suggesting aggregated structures; see ref 9.

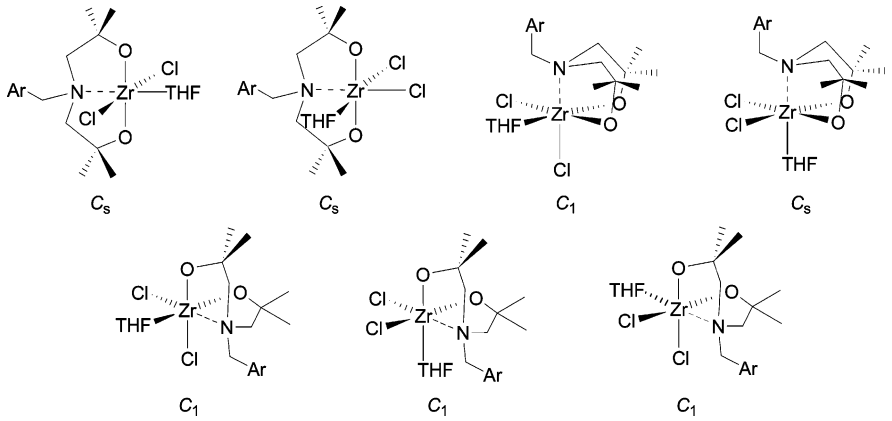

Figure 13. Some plausible structures for mononuclear {ONO^{Me}}ZrCl$_2$(THF) (**10**) (not considering isomers resulting from inversion at nitrogen).

Table 8. Ethylene Polymerization Data[a]

entry	catalyst precursor	activator (equiv)	time (min)	yield (g)	activity[b] (kgPE·mol^{-1}·h^{-1})	M_w[c] (10^{-3})	M_w/M_n[c]	T_m[d] (°C)
1	{ONO^{Me}}TiCl$_2$ (**13**)	MAO (500)	5	0.018	4.4	nd	nd	130.0
2	{ONO^{Me}}TiCl$_2$ (**13**)	MAO (500)	40	0.646	4.7	606	100	135.1
3	{ONO^{tol}}TiCl$_2$ (**14**)	MAO (500)	5	0.025	5.0	136	7.1	132.7
4	{ONO^{tol}}TiCl$_2$ (**14**)	MAO (500)	30	0.473	8.1	625	6.5	134.2
5	{ONO^{Me}}ZrCl$_2$ (**9**)	MAO (500)	0.08	0.088	1780	262	2.4	138.4
6	{ONO^{Me}}ZrCl$_2$ (**9**)	[Ph$_3$C][B(C$_6$F$_5$)$_4$] (3)/ Al(*i*Bu)$_3$ (10)	0.08	0.070	1415	375	5.4	141.4
7	{ONO^{Me}}ZrCl$_2$(THF) (**10**)	MAO (500)	30	0.000	0			
8	{ONO^{Me}}ZrCl$_2$(THF) (**10**)	[Ph$_3$C][B(C$_6$F$_5$)$_4$] (3)/ Al(*i*Bu)$_3$ (10)	30	0.000	0			
9[e]	{ONO^{Me}}Zr(CH$_2$Ph)$_2$ (**8**)	B(C$_6$F$_5$)$_3$ (1)	30	0.000	0			
10	{ONO^{Me}}Zr(CH$_2$Ph)$_2$ (**8**)	[Ph$_3$C][B(C$_6$F$_5$)$_4$] (1)	30	0.000	0			

[a] Polymerization experiments were conducted under 5 atm of ethylene using 30−140 μmol of catalyst precursor in 30−80 mL of toluene; the results shown for each entry are representative of at least two reproducible runs. [b] Average activity calculated over the whole polymerization time. [c] Determined by GPC. [d] Determined by DSC. [e] Conducted in the presence of 100 equiv of Al(*i*Bu)$_3$ as scavenger.

^{13}C NMR spectra of **10c′** feature resonances for equivalent N*CH*$_2$CMe$_2$, NCH$_2$C*Me*$_2$, and N*CH*$_2$Ph groups, reflecting a high-symmetry structure on the NMR time scale. Because dimerization/aggregation is less probable for six-coordinate species, as we observed for the related species {OSO^{Me}}TiCl$_2$(THF)$_2$ and {OSO^{Me}}ZrCl$_2$(THF)$_2$,[9] and obviously less probable in a strongly coordinating solvent such as THF, we reasonably assume that the different species observed both in benzene (**10a**, **10b**) and in THF (**10a′**, **10b′**, **10c′**) are all mononuclear isomers. Possible structures are depicted in Figure 13.

Ethylene Polymerization. The prepared complexes were briefly investigated in ethylene polymerization. Neutral {ONO^{R}}MCl$_2$(THF)$_n$ complexes **9**, **10**, **13**, and **14** were activated with MAO or a combination of [Ph$_3$C][B(C$_6$F$_5$)$_4$] with Al(*i*Bu)$_3$,[29] while molecular Lewis acidic activators were used to generate cationic benzylzirconium species from **8** in situ. The results are summarized in Table 8.

Titanium complexes **13** and **14** activated by MAO in toluene solution are poorly active for ethylene polymerization (entries 1−4).[30] No discoloration of the pale orange-yellow reaction mixture was observed over 40 min and ethylene consumption continued over this period,[31] suggesting that the active species are quite stable under these conditions. The nature of the R substituent in these {OCR$_2$CH$_2$N(CH$_2$Ph)CH$_2$CR$_2$O}-Ti systems had a minor influence on polymerization performance under the conditions investigated, as judged by the similarity of apparent activities, molecular weights, and melting points. The molecular weight of polyethylene increased over the reaction time, while the molecular weight distribution and melting points remained almost constant (entries 3 and 4).

Catalysts based on the THF-free complex {ONO^{Me}}-ZrCl$_2$ (**9**) are much more active than {ONO^{R}}-Ti catalysts but deactivate very fast (entries 5 and 6). Under the conditions investigated, all of the polyethylene is formed within 5 s, and no more ethylene is consumed after this time. Minor changes in polymerization activity and polymer characteristics arose on changing the nature of the activator. The apparent activity of systems based on **9** is higher than those reported for related catalysts based on discrete zirconium precursors having amino-alkoxide or amino-dialkoxide ligands,[32] although direct comparisons are difficult due to differences in polymerization time and conditions. In contrast, the THF-adduct {ONO^{Me}}ZrCl$_2$(THF) (**10**) (entry 6) gave no activity, whatever the activation procedure, suggesting

(29) (a) Chien, J. C. W.; Xu, B. *Makromol. Chem. Rapid Commun.* **1993**, *14*, 109−114. (b) Chien, J. C. W.; Tsai, W. M. *Makromol. Chem. Macromol. Symp.* **1993**, *66*, 141−155. (c) Chen, Y. X.; Rausch, M. D.; Chien, J. C. W. *Organometallics* **1994**, *13*, 748−749. (d) Chien, J. C. W.; Rausch, M. D. *J. Polym. Sci. Part A: Polym. Chem.* **1994**, *32*, 2387−2393. (e) Song, F. S.; Cannon, R. D.; Lancaster, S. J.; Bochmann M. *J. Mol. Catal. A* **2004**, *218*, 21−28.

(30) Eisen and co-workers have reported that the Ti[Py{CPh$_2$O)$_2$]-Cl$_2$/MAO combination exhibits modest ethylene polymerization activity (20 °C, 1 atm); see ref 5.

(31) In these experiments, polyethylene was recovered in virtually the same amount as that of ethylene consumed; oligomers (if any) are therefore negligible.

that THF could act as poison. Also, no activity was observed with discrete in situ-generated ionic zirconium-benzyl species (entries 9 and 10). Berg[6] and Kress[7] observed similar insignificant or no ethylene polymerization activity with $[RN\{CH_2CH_2C(O)R'_2\}_2]Zr(CH_2Ph)_2/B(C_6F_5)_3$ and $Zr(CH_2Ph)_2$(2,6-bis{menthoxo}pyridyl)/$B(C_6F_5)_3$ combinations, respectively, and attributed it to the formation of tight ion pairs.

The polyethylenes produced under these conditions have relatively high molecular weights and melting temperatures, indicative of essentially linear long chain microstructures. The molecular weight distributions were generally broad,[32] especially for Ti systems, although all of them feature monomodal shapes (see Supporting Information).

Conclusions

A variety of soluble chloro, alkoxy, amido, and benzyl $\{ONO^R\}MX_2$ complexes of Zr and Ti based on the new tridentate ligand system $\{OCR_2CH_2N(CH_2Ph)CH_2CR_2O\}^{2-}$, as well as bis-ligand complexes, have been prepared. The routes employed proved to be effective with both ligands bearing either methyl or *p*-tolyl R substituents. The coordination properties of these simple neutral group 4 complexes $\{ONO^R\}MX_2$ have been investigated in the solid state and in solution and compared to related systems that vary in the nature of the heteroatom donor and/or size of the metalacycles. Notably, most of the $\{ONO^{Me}\}MX_2$ complexes studied, which derived from the methyl-substituted ligand system, adopt mononuclear structures in the solid state and in solution, despite the modest steric crowding of the ligand. Also, the nature of the R substituents affects strongly the fluxional behavior of the complexes.[6]

The coordination of the nitrogen atom on metal centers in $\{ONO^R\}MX_2$ complexes, even those bearing bulky *p*-tolyl substituents, has been established unambiguously. These results cut short the proposed noncoordination of nitrogen in related amino-dialkoxide titanium complexes, suggested from MM2 computations.[10a,11a] The effective N···metal interaction in $\{ONO^R\}MX_2$ complexes seems not to decrease too dramatically the metal Lewis acidity, as demonstrated by the high ethylene polymerization activity with some $\{ONO^R\}$-$ZrCl_2$/MAO combinations. As anticipated, however, the activity of the $\{ONO^R\}ZrCl_2$/MAO combinations is somewhat lower than that observed with the parent systems $\{OSO^R\}ZrCl_2$/MAO derived from the less-donating sulfur-bridged ligands $\{OCR_2CH_2SCH_2CR_2O\}^{2-}$.[9] Reasons for the high instability of the $\{ONO^R\}ZrCl_2$/MAO catalysts, also observed with the parent $\{OSO^R\}$-M systems, are still unclear. Current investigations are directed toward understanding of these phenomena, assessing in particular possible transfer of $\{OXO^R\}^{2-}$ ligands between group 4 metal and Al centers.

(32) (a) $[RN\{CH_2CH_2C(O)R'_2\}_2]Zr(CH_2Ph)_2$/MAO (1:500) gave at 50 °C, 5 atm 136−384 kg PE·mol^{-1}·h^{-1} with M_w = 143−452 000, M_w/M_n = 3.4−5.7; see ref 6a. (b) $Zr[PyC(CF_3)_2O]_2[CH_2Ph]_2$/MAO (1:1000) gave at 30 °C, 8 atm 10 kg PE·mol^{-1}·h^{-1} with M_w = 375 000, M_w/M_n = 28; $Zr[PyC(CF_3)_2O]_2[CH_2Ph]_2/B(C_6F_5)_3$ (1:1) gave at 40 °C, 3 atm 96 kg PE·mol^{-1}·h^{-1} with M_w = 16 000, M_w/M_n = 2.6. Tsukahara, T.; Swenson, D. C.; Jordan, R. F. *Organometallics* **1997**, *16*, 3303−3313. (c) Combinations of $Zr(CH_2Ph)_2$(2,6-bis{menthoxo}pyridyl) with MAO or $B(C_6F_5)_3$ are not active for ethylene polymerization at 20 °C, 1−6 atm; see ref 7.

Experimental Section

General Considerations. All manipulations were performed under a purified argon atmosphere using standard high-vacuum Schlenk techniques or in a glovebox. Solvents (toluene, pentane, THF, diethyl ether) were freshly distilled from Na/K alloy under nitrogen and degassed thoroughly by freeze−thaw−vacuum cycles prior to use. Deuterated hydrocarbon solvents (>99.5% D, Eurisotop) were freshly distilled from sodium/potassium amalgam under argon and degassed prior to use. Ethyl *N*-benzyl(ethoxycarbonyl)methylaminoacetate was prepared according to the literature.[13] Zirconium and titanium precursors $ZrCl_4$, $Zr(OtBu)_4$, $TiCl_4$, and $Ti(OiPr)_4$ were purchased from Aldrich and were used as received. $Zr(CH_2Ph)_4$ was prepared following the literature procedure.[33] $\{Ph_3C\}\{B(C_6F_5)_4\}$ (Boulder) and MAO (30 wt % solution in toluene, Albermale) were used as received. $B(C_6F_5)_3$ (Boulder) was sublimed twice before use.

NMR spectra of complexes were recorded on Bruker AC-200, AC-300, DRX-400, DRX-500, and AM-500 spectrometers at ambient probe temperature (23 °C) unless otherwise indicated. ^1H and ^{13}C chemical shifts are reported in ppm vs $SiMe_4$ and were determined by reference to the residual solvent peaks. Assignment of signals was made from $^1H-^1H$ COSY, $^1H-^{13}C$ HMQC, and HMBC NMR experiments (the markers a, b, ..., in assignments of NMR data refer to bound H and C atoms). NMR probe temperatures were calibrated by a MeOH thermometer.[34] All coupling constants are given in hertz. Elemental analyses were performed by the Microanalytical Laboratory at the Institute of Chemistry of Rennes and are the average of two independent determinations. Melting points are uncorrected.

Gel permeation chromatography (GPC) was performed on a Polymer Laboratories PL-GPC 220 instrument using 1,2,4-trichlorobenzene solvent (stabilized with 125 ppm BHT) at 150 °C. A set of three PLgel 10 μm Mixed-B or Mixed-B LS columns was used. Samples were prepared at 160 °C. Polyethylene molecular weights were determined vs polystyrene standards and are reported relative to polyethylene standards, as calculated by the universal calibration method using Mark−Houwink parameters ($K = 14.1 \times 10^{-5}$, $\alpha = 0.70$ for PSt, $K = 14.1 \times 10^{-5}$, $\alpha = 0.70$ for PE).[35] DSC measurements were performed on a TA Instruments DSC 2920 differential scanning calorimeter. Polyethylene samples (10 mg) were annealed by heating to 170 °C at 20 °C/min, followed by cooling to 40 °C at 40 °C/min, then heating to 170 °C at 20 °C/min.

$\{ONO^{Me}\}H_2$ (1). A solution of isobutene oxide (3.00 g, 41.6 mmol) and benzylamine (1.11 g, 10.4 mmol) in methanol (50 mL) was heated under reflux for 15 days. The mixture was cooled to room temperature and filtered. The white powder collected was dissolved in CH_2Cl_2 (30 mL) and dried for 48 h over $MgSO_4$. After filtration, volatiles were removed under vacuum, leaving **1** as a white powder (2.61 g, 98%). Mp = 95 °C. Anal. Calcd for $C_{15}H_{25}NO_2$: C, 71.67; H, 10.02; N, 5.57. Found: C, 71.29; H, 10.06; N, 5.47. ^1H NMR (C_6D_6, 500 MHz): δ 7.36 (d, 2H, ^2J = 7.5 Hz, *o*-H), 7.28 (t, 2H, 7.3 Hz, *m*-H), 7.21 (t, 1H, 7.2 Hz, *p*-H), 4.59 (s, 2H, OH), 3.70 (s, 2H, NCH_2Ph), 2.70 (s, 4H, NCH_2CMe_2), 1.24 (s, 12H, CH_3). ^1H NMR ($CDCl_3$, 200 MHz): δ 7.32−7.40 (m, 5H, phenyl), 3.77 (s, 2H, NCH_2Ph), 3.46 (s, 2H, OH), 2.66 (s, 4H, NCH_2CMe_2), 1.13 (s, 12H, CH_3). ^1H NMR (THF-d_8, 200 MHz): δ 7.02−7.17 (m, 5H, phenyl), 3.76 (s, 2H, OH), 3.43 (s, 2H, NCH_2Ph), 2.58 (s, 4H, NCH_2CMe_2), 1.09 (s, 12H, CH_3). $^{13}C\{^1H\}$ NMR (C_6D_6, 125 MHz): δ 140.1 (*ipso*-C), 129.1 (*o*-C), 128.2 (*m*-C), 127.0 (*p*-C), 71.6 (NCH_2CMe_2), 68.1 (NCH_2CMe_2), 64.0 (NCH_2Ph), 27.9 (Me).

(33) Zucchini, U.; Albizzati, E.; Giannini, U. *J. Organomet. Chem.* **1971**, *26*, 357−372.

(34) Van Geet, A. L. *Anal. Chem.* **1970**, *42*, 679−680.

(35) Scholte, Th. G.; Meijerink, N. L. J.; Schofelleers, H. M.; Brands, A. M. G. *J. Appl. Polym. Sci.* **1984**, *29*, 3763−3782.

{ONO^{tol}}H$_2$ (2). Et_2O (50 mL) and a few drops of CH_3I were introduced in a Schlenk flask containing magnesium turnings (2.27 g, 97.5 mmol) under argon. After a pale yellow color appeared, 4-bromotoluene (8.00 g, 48.8 mmol) was added dropwise to maintain gentle ebullition of the mixture. The mixture was stirred at room temperature for 4 h. The Grignard solution was filtered and titrated with a 1.0 M solution of 2-butanol in toluene in the presence of *o*-phenantroline, indicating a 90% yield. The solution was cooled to −5 °C, and ethyl (*N*-benzylethoxycarbonylmethylamino)acetate (1.95 g, 7.0 mmol) was added by portion over 1 h. The mixture was refluxed for 2 h, then cooled to 0 °C and quenched with an aqueous solution of NH_4Cl (20 mL of a 2.15 mol/L solution, 43 mmol). The aqueous phase was washed with ether (3 × 20 mL), and the organic phase was washed with water (2 × 10 mL). The organic phases were combined and dried over $MgSO_4$ for 24 h. After filtration, volatiles were removed under vacuum and the resulting white powder was recrystallized from ethanol to yield **2** as a colorless microcrystalline powder (1.80 g, 47%). Mp = 177 °C. Anal. Calcd for $C_{39}H_{41}NO_2$: C, 84.29; H, 7.44; N, 2.52. Found: C, 84.36; H, 7.51; N, 2.61. ^{1}H NMR ($CDCl_3$, 300 MHz): δ 7.17 (d, ^3J = 8.2 Hz, 8H, *p*-tol), 6.16−6.91 (m, 5H, Ph), 7.05 (d, ^3J = 8.2 Hz, 8H, *p*-tol), 4.28 (s, 2H, OH), 3.58 (s, 4H, NCH_2C(*p*-tol)$_2$), 3.32 (s, 2H, NCH_2Ph), 2.30 (s, 12H, CH_3, *p*-tol). ^{1}H NMR (toluene-d_8, 500 MHz): δ 7.33 (d, ^3J = 8.2 Hz, 8H, *p*-tol), 7.15−6.91 (m, 5H, Ph), 6.92 (d, ^3J = 8.2 Hz, 8H, *p*-tol), 4.50 (s, 2H, OH), 3.62 (s, 4H, NCH_2C(tol)$_2$), 3.34 (s, 2H, NCH_2Ar), 2.12 (s, 12H, CH_3, *p*-tol). ^{13}C{^{1}H} NMR (toluene-d_8, 125 MHz): δ 143.8 (*ipso*-C, *p*-tol), 138.5 (*ipso*-C, Ph), 135.7 (*p*-C, *p*-tol), 129.8 (*o*-C, *p*-tol), 128.8 (*m*-C, Ph), 128.1 (*m*-C, *p*-tol), 127.9 (*o*-C, Ph), 127.0 (*p*-C, Ph), 77.3 (NCH_2C(*p*-tol)$_2$), 65.6 (NCH_2C(*p*-tol)$_2$), 61.8 (CH_2Ph), 20.5 (CH_3 *p*-tol).

{ONO^{Me}}Ti(O*i*Pr)$_2$ (3). A solution of **1** (0.250 g, 0.879 mmol) in toluene (3 mL) at −30 °C was added dropwise over 5 min to a stirred solution of Ti(O*i*Pr)$_4$ (0.274 g, 0.879 mmol) in toluene (2 mL) at −30 °C. Stirring was maintained for 5 h, letting the mixture warm to room temperature. Removal of volatiles under vacuum left a white powder, which was recrystallized from pentane at −30 °C to give **3** as colorless crystals (0.355 g, 87%). Anal. Calcd for $C_{21}H_{37}O_4NTi$: C, 60.72; H, 8.92; N, 3.37. Found: C, 60.29; H, 8.97; N, 3.42. ^{1}H NMR (toluene-d_8, 500 MHz, 320 K): δ 7.22−7.16 (m, 5H, phenyl), 4.85 (sept, ^3J = 6.1 Hz, 2H, CH (O*i*Pr)), 4.39 (s, 2H, CH_2Ar), 2.84 (s, 4H, CH_2NCMe$_2$), 1.40 (d, ^3J = 6.1 Hz, 12H, CH_3 (O*i*Pr)), 1.30 (s, 12H, CH_3). ^{1}H NMR (toluene-d_8, 500 MHz, 252 K): δ 7.24−7.16 (m, 5H, phenyl), 4.93 (sept, ^3J = 4.4 Hz, 2H, CH (OiPr)), 4.40 (s, 2H, CH_2Ph), 3.05 (d, ^2J = 12.7 Hz, 2H, C*HH*NCMe$_2$), 2.42 (d, ^2J = 12.7 Hz, 2H, C*HH*NCMe$_2$), 1.48 (d, ^3J = 4.4 Hz, 6H, CH_3 (O*i*Pr)), 1.44 (d, ^2J = 4.4 Hz, 6H, CH_3 (O*i*Pr)), 1.42 (s, 6H, CH_3), 1.24 (s, 6H, CH_3). ^{13}C{^{1}H} NMR (toluene-d_8, 125 MHz, 320 K): δ 135.7 (ipso, Ph), 131.0 and 128.1 (*o*- and *m*-C, Ph), 127.5 (*p*-C, Ph), 81.4 (NCH_2C(Me)$_2$), 76.0 (CH (O*i*Pr)), 68.7 (NCH_2C(Me)$_2$), 63.6 (CH_2Ph), 31.1 (CH_3 (O*i*Pr)), 27.9 (CH_3).

Reaction of Zr(O*t*Bu)4 with Diol 1: Generation of {ONO^{Me}}Zr(O*t*Bu)$_2$ (4) and {ONO^{Me}}$_2$Zr (6). This reaction was carried out as described above for the synthesis of **3** starting from **1** (0.100 g, 0.39 mmol) and Zr(O*t*Bu)$_4$ (0.148 g, 0.39 mmol). Workup afforded a white powder, which was recrystallized from pentane at −30 °C to give a mixture of colorless crystals of **4** and **6** (0.172 g), in a 1:2 ratio according to ^{1}H NMR. Further crystallization did not allow recovering **4** in an analytically pure form. Complex **4**: ^{1}H NMR (THF-d_8, 300 MHz): δ 7.49−7.34 (m, 5H, phenyl), 4.32 (s, 2H, CH_2Ar), 2.87 (s, 4H, CH_2NCMe_2), 1.27 (s, 12H, CH_3), 1.25 (s, 18H, O*t*Bu). ^{13}C{^{1}H} NMR (THF-d_8, 75 MHz): δ 138.1 (*ipso*-C, Ph), 130.2 (*o*-C, Ph), 128.0 and 127.1 (*p*- and *m*-C), Ph), 78.2 (O*C*(CH$_3$)$_2$), 72.9 (*C*(CH$_3$)$_3$), 62.1 (NCH_2Ph), 52.2 (NCH_2), 33.0 (C(*C*H$_3$)$_3$), 31.0 (OC(*C*H$_3$)$_2$).

{ONO^{Me}}$_2$Ti (5). This complex was prepared as described above for **3** starting from **1** (0.300 g, 1.19 mmol) and Ti(O*i*Pr)$_4$ (0.170 g, 0.59 mmol). Workup afforded **4** as a white powder (0.282 g, 86%). Anal. Calcd for $C_{30}H_{46}N_2O_4Ti$: C, 65.92; H, 8.48; N, 5.13. Found: C, 66.26; H, 8.57; N, 5.08. ^{1}H NMR (toluene-d_8, 300 MHz, 298 K): δ 7.23−7.18 (m, 10H, phenyl), 4.25 (s, 4H, CH_2Ph), 2.83 (s, 8H, CH_2NCMe$_2$), 1.37 (s, 24H, CH_3). ^{1}H NMR (toluene-d_8, 300 MHz, 193 K): δ 7.35−7.20 (m, 10H, phenyl), 4.69 (d, ^2J = 9.0 Hz, 2H, C*HH*Ph), 4.12 (d, ^2J = 9.0 Hz, 2H, C*HH*Ph), 3.08 (d, ^2J = 7.9 Hz, 1H, C*HH*NCMe$_2$), 2.85 (d, ^2J = 7.9 Hz, 1H, C*HH*NCMe$_2$), 2.53 (d, ^2J = 7.9 Hz, 1H, C*HH*NCMe$_2$), 2.35 (d, ^2J = 7.9 Hz, 1H, C*HH*NCMe$_2$), 1.87 (s, 3H, CH_3), 1.57 (s, 3H, CH_3), 1.32 (s, 3H, CH_3), 1.21 (s, 3H, CH_3). ^{3}C{^{1}H} NMR (toluene-d_8, 75 MHz, 298 K): δ 137.1 (*ipso*-C, Ph), 130.5 and 128.1 (*o*- and *m*-C, Ph), 127.3 (*p*-C, Ph), 81.7 (NCH_2C(Me)$_2$), 68.3 (NCH_2C(Me)$_2$), 63.6 (CH_2Ph), 27.9 (CH_3). ^{13}C{^{1}H} NMR (toluene-d_8, 300 MHz, 203 K): δ 136.6 (*ipso*, Ph), 131.3 and 128.4 (*o*- and *m*-C, Ph), 127.7 (*p*-C, Ph), 81.7 (NCH_2C(Me)$_2$), 80.8 (NCH_2C(Me)$_2$), 69.3 (NCH_2C(Me)$_2$), 64.9 (NCH_2C(Me)$_2$), 63.8 (CH_2Ph), 32.0 (CH_3), 30.7 (2C, 2 CH_3), 29.7 (CH_3).

{ONO^{Me}}$_2$Zr (6). This complex was prepared as described above for **3** starting from **1** (0.400 g, 1.54 mmol) and Zr(O*t*Bu)$_4$ (0.296 g, 0.77 mmol). Workup afforded **5** as a white powder (0.361 g, 80%). Anal. Calcd for $C_{30}H_{46}N_2O_4Zr$: C, 61.08; H, 7.87; N, 4.75. Found: C, 62.77; H, 8.42; N, 4.65. ^{1}H NMR (THF-d_8, 500 MHz): δ 7.49−7.34 (m, 5H, phenyl), 4.39 (s, 2H, CH_2Ar), 2.94 (s, 4H, CH_2NCMe_2), 1.34 (s, 12H, CH_3). ^{1}H NMR (toluene-d_8, 500 MHz, 243 K): δ 7.48−7.18 (m, 5H, phenyl), 4.74 (d, ^2J = 15.0 Hz, 1H, C*HH*Ph), 4.28 (d, ^2J = 15.0 Hz, 1H, C*HH*Ph), 3.09 (d, ^2J = 13.3 Hz, 1H, C*HH*NCMe$_2$), 2.96 (d, ^2J = 13.3 Hz, 1H, C*HH*NCMe$_2$), 2.64 (d, ^2J = 13.3 Hz, 1H, C*HH*NCMe$_2$), 2.53 (d, ^2J = 13.3 Hz, 1H, C*HH*NCMe$_2$), 1.60 (s, 3H, CH_3), 1.42 (s, 3H, CH_3), 1.36 (s, 3H, CH_3), 1.25 (s, 3H, CH_3). ^{1}H NMR (toluene-d_8, 500 MHz, 340 K): δ 7.17−7.32 (m, 5H, phenyl), 4.48 (s, 2H, CH_2Ph), 2.89 (s, 4H, CH_2NCMe_2), 1.36 (s, 12H, CH_3). ^{13}C{^{1}H} NMR (toluene-d_8, 125 MHz, 330 K): δ 137.74 (*ipso*, Ph), 131.19 (*o*-C, Ph), 128.1 and 127.5 (*p*- and *m*-C, Ph), 77.1 (NCH_2C(Me)$_2$), 68.4 (NCH_2C(Me)$_2$), 63.0 (CH_2Ph), 32.2 (CH_3).

{ONO^{tol}}$_2$Zr (7). This complex was prepared as described above for **3** starting from **2** (0.100 g, 0.18 mmol) and Zr(O*t*Bu)$_4$ (0.034 g, 0.090 mmol). Workup afforded a white powder, which was recrystallized from pentane at −30 °C to give colorless crystals of **7** (0.110 g, 91%). Anal. Calcd for $C_{78}H_{78}N_2O_4Zr$: C, 78.15; H, 6.56; N, 2.34. Found: C, 78.38; H, 6.43; N, 2.24. ^{1}H NMR (toluene-d_8, 500 MHz): δ 7.90 (d, ^3J = 7.3 Hz, 4H, *o*-H *p*-tol), 7.63 (d, ^3J = 7.3 Hz, 4H, *o*-H *p*-tol), 7.50 (d, ^3J = 7.3 Hz, 4H, *o*-H *p*-tol), 7.34 (d, ^3J = 7.1 Hz, 4H, *o*-H *p*-tol), 7.10−7.20 (m, 10H, *m*-H Bz, *p*-H Bz and *m*-H ptol), 6.91 (d, ^3J = 8.0 Hz, 4H, *m*-H *p*-tol), 6.86−6.84 (m, 8H, *o*-H Bz and *m*-H *p*-tol), 6.82 (d, ^3J = 8 Hz, 4H, *m*-H *p*-tol), 4.79 (d, ^2J = 14.2 Hz, 2H, C*HH*Ph), 4.63 (d, ^2J = 14.2 Hz, 2H, C*HH*Ph), 4.03 (d, ^2J = 12.7 Hz, 2H, NC*HH*C(*p*-tol)$_2$), 4.01 (d, ^2J = 12.7 Hz, 2H, NC*HH*C(*p*-tol)$_2$), 3.91 (d, ^2J = 12.7 Hz, 2H, NC*HH*C(*p*-tol)$_2$), 3.75 (d, ^2J = 12.7 Hz, 2H, NC*HH*C(*p*-tol)$_2$), 2.24 (s, 6H, CH_3 *p*-tol), 2.20 (s, 12H, 2 CH_3 *p*-tol), 2.00 (s, 6H, CH_3 *p*-tol). ^{13}C-{^{1}H} NMR (toluene-d_8, 125 MHz, 298 K): δ 149.0 (*ipso*-C, *p*-tol), 148.3 (*ipso*-C, *p*-tol), 147.9 (*ipso*-C, *p*-tol), 147.1 (*ipso*-C, *p*-tol), 134.9 (*p*-C, *p*-tol), 134.6 (*p*-C, *p*-tol), 134.5 (*p*-C, *p*-tol), 134.1 (*ipso*-C, bz), 134.0 (*p*-C, *p*-tol), 131.19 (*o*-C, bz), 128.7 and 128.4 (*m*-C, *p*-tol), 128.3 and 128.2 (*m*-C and *p*-C, bz), 85.4 (NCH_2C(Me)$_2$), 84.8 (NCH_2C(Me)$_2$), 66.7 (NCH_2C(Me)$_2$), 66.3 (NCH_2C(Me)$_2$), 60.3 (CH_2Ph), 20.7 (CH_3), 20.6 (CH_3), 20.4 (2 overlapping signals, 2 CH_3).

{ONO^{Me}}Zr(CH$_2$Ph)$_2$ (8). Synthesis by Alkane Elimination. A solution of **1** (0.200 g, 0.795 mmol) in toluene (20 mL) was added at −20 °C to a solution of Zr(CH$_2$Ph)$_4$ (0.354 g, 0.795 mmol) in toluene (20 mL). The mixture was stirred for 2 h at room temperature. The clear solution was concentrated under vacuum to ca. 1/4 of the initial volume and placed at −30 °C to afford **8** as a colorless microcrystalline powder (0.380 g, 91%). Anal. Calcd for $C_{29}H_{37}NO_2Zr$: C, 66.62; H, 7.13; N, 2.68.

Found: C, 66.21; H, 7.01; N, 2.59. ^{1}H NMR (toluene-d_8, 500 MHz, 295 K): δ 7.14−6.95 (m, 15H, Ar), 3.56 (s, 2H, NCH_2-Ar), 3.14 (d, ^2J = 13.5 Hz, 2H, NC*HH*), 2.34 (s, 2H, CH_2Ar-(a)), 2.05 (d, ^2J = 13.5 Hz, 2H, NC*HH*), 1.76 (s, 2H, CH_2Ar(b)), 1.43 (s, 6H, CH_3), 1.15 (s, 6H, CH_3). ^{1}H NMR (toluene-d_8, 500 MHz, 375 K): δ 7.07−6.95 (m, 15H, Ar), 3.58 (s, 2H, NCH_2-Ar), 2.66 (s, 4H, NCH_2), 2.04 (s, 4H, ZrCH_2), 1.19 (s, 12H, CH_3). ^{13}C{^{1}H} NMR (toluene-d_8, 125 MHz, 295 K): δ 147.3 (*ipso*-C(b)), 141.4 (*ipso*-C(a)), 138.3, 132.2, 129.6 (*o*-C(b)), 129.0 (*o*-C(a)), 122.3 (*p*-C(a)), 121.3 (*p*-C(b)), δ 82.8 (s, C), 69.1 (N*C*H_2), 55.1 (*C*H_2Ar(b)), 54.3 (*C*H_2Ar(a)), 53.3 (N*C*H_2Ar), 34.1 (CH_3), 32 (CH_3).

Synthesis by Comproportionation. Zr(CH_2Ph)$_4$ (0.042 g, 0.167 mmol) and **6** (0.076 g, 0.167 mmol) were introduced in a Teflon-valved NMR tube, and toluene-d_8 (ca. 1.5 mL) was vacuum-transferred in at −180 °C. The tube was sealed and warmed to room temperature. ^{1}H NMR spectroscopy revealed 90% conversion of the starting reagents to **8**.

{ONO^{Me}}ZrCl$_2$ (9). Synthesis by Alkane Elimination from "Zr(*n*-Bu)$_2$Cl$_2$". *n*-BuLi (3.5 mL of a 1.6 M solution in hexane, 5.62 mmol) was added dropwise, over 10 min, to a stirred solution of $ZrCl_4$ (0.656 g, 2.81 mmol) in toluene (15 mL) at −78 °C. The mixture was slowly warmed to room temperature and stirred for 8 h, resulting in a brown slurry. This mixture of "Zr(*n*-Bu)$_2$Cl$_2$" and LiCl was cooled at −40 °C, and a solution of diol **1** (0.708 g, 2.81 mmol) in toluene (5 mL) was added dropwise under stirring over 30 min. The brown mixture was slowly warmed to room temperature and stirred for 8 h. Gas evolution (butane) was observed without change in the color. The precipitate (LiCl) was removed by filtration over a frit and washed with toluene (2 × 30 mL). The filtrate was concentrated under vacuum to leave a white powder, which was washed with pentane (2 × 5 mL) and dried under vacuum (0.656 g, 56%). This product was very poorly soluble in toluene and readily soluble in THF.

Synthesis via Comproportionation of ZrCl$_4$ and {ONO^{Me}}$_2$Zr. In the glovebox, a solution of complex **6** (0.050 g, 0.085 mmol) in toluene (2 mL) and a solution of $ZrCl_4$ (0.020 g, 0.085 mmol) in toluene (2 mL) were cooled at −30 °C and rapidly mixed. The mixture was stirred at room temperature for 24 h. Volatiles were removed under vacuum to leave **9** as a white powder (0.069 g, 100%). Anal. Calcd for $C_{15}H_{23}Cl_2NO_2Zr$: C, 43.78; H, 5.63; N, 3.40. Found: C, 44.12; H, 5.48; N, 3.20. This product was sparingly soluble in toluene and readily soluble in THF. ^{1}H NMR spectroscopy of **9** in toluene indicated it is a mixture of isomers of which two major ones, **9a** and **9b**, account for more than 80% of the total, with a ratio **9a/9b** = 53:47. Isomer **9a**: ^{1}H NMR (toluene-d_8, 500 MHz): δ 7.28−7.01 (m, 5H, phenyl), 4.00 (m, 2H, C*HH*Ar), 2.88 (m, 4H, C*HH*NCMe$_2$), 1.38 (s, 12H, CH_3). Isomer **9b**: ^{1}H NMR (toluene-d_8, 500 MHz): δ 7.28−7.01 (m, 5H, phenyl), 4.71 (d, ^2J = 15.2 Hz, 1H, C*HH*Ar), 4.53 (d, ^2J = 15.2 Hz, 1H, C*HH*Ar), 3.32 (d, ^2J = 13.1 Hz, 1H, C*HH*NCMe$_2$), 3.05 (d, ^2J = 13.1 Hz, 1H, C*HH*NCMe$_2$), 2.87 (d, ^2J = 13.1 Hz, 1H, C*HH*NCMe$_2$), 2.65 (d, ^2J = 13.1 Hz, 1H, C*HH*NCMe$_2$), 2.02 (s, 3H, CH_3), 1.78 (s, 3H, CH_3), 1.39 (s, 3H, CH_3), 1.37 (s, 3H, CH_3). ^{1}H NMR spectroscopy of **9** in THF-d_8 indicated a mixture of isomers, of which three major ones, **10a′**, **10b′**, and **10c′**, account for more than 90% of the total, with a ratio **10a′/10b′/10c′** = 30:7:63.

{ONO^{Me}}ZrCl$_2$(THF) (10). Synthesis by Salt Elimination. *n*-BuLi (2.49 mL of a 1.6 M solution in hexane, 3.98 mmol) was added dropwise, under stirring, to a solution of **1** (0.500 g, 1.99 mmol) in THF (7 mL) at −78 °C. The mixture was warmed to room temperature and stirred for 24 h. It was then cooled at −40 °C and slowly transferred over 30 min into a solution of $ZrCl_4$ (0.463 g, 1.99 mmol) in THF (3 mL) at −40 °C (previously prepared 3 h before addition). The mixture turned yellow upon addition of the dialkoxide and was stirred at room temperature overnight. Volatiles were removed under vacuum, and the residue was extracted with toluene (4 × 15 mL). Filtration of the solution and concentration under vacuum of the filtrate offered **10** as a white powder (0.691 g, 52%). This product was soluble in benzene, toluene, and THF. ^{1}H NMR spectroscopy of **10** in benzene-d_6 or toluene-d_8 indicated a mixture of isomers, of which two major ones, **10a** and **10b**, account for more than 80% of the total, with a ratio **10a/10b** = 70:30. Isomer **10a**: ^{1}H NMR (C_6D_6, 300 MHz): δ 7.28−7.01 (m, 5H, phenyl), 4.70 (d, ^2J = 15.2 Hz, 1H, C*HH*Ar), 4.54 (d, ^2J = 15.2 Hz, 1H, C*HH*Ar), 3.33 (m, 4H, OCH_2 THF), 3.29 (d, ^2J = 13.1 Hz, 1H, C*HH*NCMe$_2$), 2.99 (d, ^2J = 13.1 Hz, 1H, C*HH*NCMe$_2$), 2.86 (d, ^2J = 13.1 Hz, 1H, C*HH*NCMe$_2$), 2.61 (d, ^2J = 13.1 Hz, 1H, C*HH*NCMe$_2$), 2.01 (s, 3H, CH_3), 1.79 (s, 3H, CH_3), 1.71 (m, 4H, CH_2CH_2 THF), 1.40 (s, 3H, CH_3), 1.36 (s, 3H, CH_3). ^{13}C{^{1}H} NMR (C_6D_6, 125 MHz): δ 133.8 (*ipso*-C), 81.2 (*C*(CH_3)$_2$), 80.2 (*C*(CH_3)$_2$), 71.7 (NCH_2(CH_3)$_2$), 70.6 (O*C*H_2, THF), 66.2 (NCH_2(CH_3)$_2$), 60.6 (N*C*H_2Ar), 32.6 (CH_3), 31.2 (CH_3), 28.0 (CH_3), 27.7 (CH_3), 26.9 (*C*H_2CH_2, THF). Isomer **10b**: ^{1}H NMR (C_6D_6, 75 MHz): δ 7.28−7.01 (m, 5H, phenyl), 4.00 (m, 2H, CH_2Ar), 3.05 (m, 4H, CH_2NCMe$_2$), 1.47 (s, 6H, CH_3), 1.36 (s, 6H, CH_3) and the same ^{1}H resonances of THF as above for **10a**. ^{13}C{^{1}H} NMR (C_6D_6, 300 MHz): δ 140.6 (*ipso*-C), 83.1 (*C*(CH_3)$_2$), 71.7 (NCH_2(CH_3)$_2$), 63.4 (NCH_2Ar), 31.2 (CH_3) and the same ^{13}C resonances of THF as above for **10a**. ^{1}H NMR spectroscopy of **10** in THF-d_8 indicated a mixture of isomers, of which three major ones, **10a′**, **10b′**, and **10c′**, account for more than 80% of the total, with a ratio **10a′/10b′/10c′** = 34:13:53. A ^{1}H NMR monitoring indicated that isomers **10a′** and **10b′** slowly convert into isomer **10c′** in THF solution at room temperature (90% conversion within 1 week). Isomer **10a′**: ^{1}H NMR (THF-d_8, 500 MHz): δ 7.47 (d, ^3J = 10.1 Hz, 2H, *o*-H), 7.41 (m, 1H, *p*-H), 7.38 (m, 2H, *m*-H), 4.72 (d, ^2J = 15.0 Hz, 1H, C*HH*Ar), 4.53 (d, ^2J = 15.0 Hz, 1H, C*HH*Ar), 3.55 (d, ^2J = 13.0 Hz, 1H, C*HH*NCMe$_2$), 3.19 (d, ^2J = 13.0 Hz, 1H, C*HH*NCMe$_2$), 3.04 (d, ^2J = 13.0 Hz, 1H, C*HH*NCMe$_2$), 2.78 (d, ^2J = 13.0 Hz, 1H, C*HH*NCMe$_2$), 1.93 (s, 3H, CH_3), 1.65 (s, 3H, CH_3), 1.59 (s, 3H, CH_3), 1.39 (s, 3H, CH_3). ^{13}C{^{1}H} NMR (THF-d_8, 500 MHz): δ 133.6 (*ipso*-C), 132.0 (*o*-C), 128.2 (*p*-C), 128.1 (*m*-C), 81.4 (*C*(CH_3)$_2$), 80.5 (*C*(CH_3)$_2$), 70.6 (NCH_2(CH_3)$_2$), 65.9 (NCH_2(CH_3)$_2$), 60.5 (NCH_2Ar), 32.2 (CH_3), 30.7 (2 CH_3), 28.8 (CH_3) (THF resonances were not clearly identified because of multiple overlapping resonances). Isomer **10b′**: ^{1}H NMR (THF-d_8, 500 MHz): δ 7.48−7.18 (m, 5H, phenyl), 3.99 (m, 2H, C*H*$_2$Ar), 2.91 (m, 4H, CH_2NCMe$_2$), 1.18 (s, 6H, CH_3), 1.22 (s, 6H, CH_3). ^{13}C{^{1}H} NMR (THF-d_8, 125 MHz): δ 140.4 (*ipso*-C), 128.6 (*o*-C), 127.2 (*p*-C), 126.8 (*m*-C), 82.5 (*C*(CH_3)$_2$), 71.4 (NCH_2(CH_3)$_2$), 63.2 (NCH_2Ar), 27.1 (CH_3). Isomer **10c′**: ^{1}H NMR (THF-d_8, 500 MHz): δ 7.48−7.18 (m, 5H, phenyl), 3.99 (s, 2H, CH_2Ar), 2.91 (s, 4H, CH_2NCMe$_2$), 1.15 (s, 12H, CH_3). ^{13}C{^{1}H} NMR (THF-d_8, 125 MHz): δ 140.4 (*ipso*-C), 128.6 (*o*-C), 127.2 (*p*-C), 126.8 (*m*-C), 82.5 (*C*(CH_3)$_2$), 71.4 (NCH_2(CH_3)$_2$), 63.2 (NCH_2Ar), 27.1 (CH_3).

{ONO^{Me}}Zr(NMe$_2$)$_2$ (11). A solution of **1** (0.245 g, 0.974 mmol) in toluene (5 mL) at −30 °C was slowly transferred to a stirred solution of Zr(NMe$_2$)$_4$ (0.261 g, 0.974 mmol) in toluene (5 mL) at −30 °C. The reaction mixture was warmed to room temperature and stirred for 48 h under partial vacuum. Volatiles were removed under vacuum, and the residue was washed with pentane (2 × 5 mL), leaving **11** as a white powder (0.381 g, 91%). Anal. Calcd for $C_{19}H_{35}N_3O_2Zr$: C, 53.23; H, 8.23; N, 9.80. Found: C, 52.87; H, 8.13; N, 9.45. ^{1}H NMR spectroscopy in toluene-d_8 at room temperature and 60 °C featured many resonances.

{ONO^{Me}}ZrCl$_2$(THF) (10). Synthesis from 11. In a Teflon-valved NMR tube containing a solution of complex **7** (0.040 g, 0.093 mmol) in THF-d_8 (1.5 mL) at −30 °C was added ClSiMe$_3$ (0.020 g, 0.018 mmol). The reaction mixture was gently warmed to room temperature, while vigorously shaken for 10 min, and then left standing for 12 h. A ^{1}H NMR spectrum showed complete and selective transformation of **11** to **10**. Volatiles were removed under vacuum, and the residue was washed with pentane and finally dried in a vacuum to afford **11** as a white powder (0.038 g, 84%). Anal. Calcd for

$C_{19}H_{31}Cl_2NO_3Zr$: C, 47.19; H, 6.46; N, 2.90. Found: C, 47.74; H, 6.56; N, 2.90. ^{1}H NMR in THF-d_8 showed the presence of three isomers, **10a′**, **10b′**, and **10c′**, in a 33:21:46 ratio.

{κ^2-ONO^{Me}}Zr(μ^2-NMe$_2$)(μ^2,κ^3-{ONO^{Me}})Zr(κ^2-{ONO^{Me}})-(NMe$_2$) (12). A small amount of X-ray quality crystals of the dimeric species **12**, which results from the exchange of two NMe_2 units by a $\{ONO^{Me}\}^{2-}$ moiety in **11**, was isolated from a toluene solution of a sample of **11** (prepared as described above) placed at −30 °C.

{ONO^{Me}}TiCl$_2$ (13). $TiCl_4$ (0.059 g, 0.315 mmol) was added dropwise at room temperature to a stirred solution of $Ti(OiPr)_4$ (0.089 g, 0.315 mmol) in toluene (2 mL). The mixture was stirred for 1 h, and a solution of **1** (0.163 g, 0.629 mmol) in toluene (3 mL), cooled at −30 °C, was added dropwise over 2 min. The mixture was stirred for 12 h at room temperature, and volatiles were removed under vacuum. The residue was washed with pentane (2 × 2 mL) and dried under vacuum to leave **13** as a white powder (0.065 g, 78%). Anal. Calcd for $C_{15}H_{23}O_2NCl_2Ti$: C, 48.94; H, 6.30; N, 3.80. Found: C. 49.49; H, 7.02; S, 3.58. ^{1}H NMR (toluene-d_8, 300 MHz, 243 K): δ 7.92−7.17 (m, 5H, aryl), 4.09 (s, 2H, CH_2Ar), 2.91 (d, ^2J = 13.4 Hz, 2H, C*HH*NCMe$_2$), 2.50 (d, ^2J = 13.4 Hz, 2H, C*HH*NCMe$_2$), 1.16 (s, 6H, CH_3), 1.06 (s, 6H, CH_3). ^{1}H NMR (toluene-d_8, 500 MHz, 340 K): δ 6.95−7.15 (m, 5H, phenyl), 4.15 (s, 2H, CH_2-Ar), 2.86 (s, 4H, C*H*$_2$NCMe$_2$), 1.16 (s, 12H, CH_3). ^{13}C{^{1}H} NMR (toluene-d_8, 75 MHz, 243 K): δ 137.0 (*ipso*-C, Ph), 133.3 and 131.5 (*o*- and *m*-C, Ph), 129.2 (*p*-C, Ph), 91.3 (NCH$_2$*C*), 68.1 (N*C*H$_2$), 65.3 (N*C*H$_2$Ph), 30.0 (CH_3).

{ONO^{tol}}TiCl$_2$ (14). This complex was prepared as described above for **13**, starting from $TiCl_4$ (0.040 g, 0.21 mmol), $Ti(OiPr)_4$ (0.059 g, 0.21 mmol), and **2** (0.232 g, 0.42 mmol). Workup afforded **14** as a white powder (0.241 g, 86%). Anal. Calcd for $C_{39}H_{39}Cl_2NO_2Ti$: C, C, 69.65; H, 5.85; N, 2.08. Found: C, 69.79; H, 5.66; N, 2.22. ^{1}H NMR (toluene-d_8, 300 MHz): δ 7.43 (d, ^3J = 8.1 Hz, 4H, *o*-H *p*-tol), 7.08−7.15 (m, 3H, *m*-H bz and *p*-H bz), 6.95 (d, ^3J = 8.1 Hz, 4H, *o*-H *p*-tol), 6.92 (d, ^3J = 8.1 Hz, 4H, *m*-H *p*-tol), 6.63 (d, ^3J = 8.1 Hz, 4H, *m*-H *p*-tol), 6.44 (d, ^3J = 6.1 Hz, 2H, *o*-H Bz), 4.09 (s, 2H, CH_2-Ar), 3.91 (d, ^2J = 12.8 Hz, 2H, NC*HH*CMe$_2$), 3.82 (d, ^2J = 12.8 Hz, 2H, NC*HH*CMe$_2$), 2.08 (s, 6H, CH_3), 2.04 (s, 6H, CH_3). ^{13}C-{^{1}H} NMR (toluene-d_8, 75 MHz): δ 143.1 (*ipso*-C, *p*-tol), 143.0 (*ipso*-C, *p*-tol), 136.8 (*p*-C, *p*-tol), 136.1 (*p*-C, *p*-tol), 133.0 (*ipso*-C, Bz), 131.5 (*o*-C, Bz), 129.0 and 128.9 (*m*-C, *p*-tol), 128.5 and 128.6 (*m*-C and *p*-C, Bz), 124.8 and 124.6 (*o*-C, *p*-tol), 97.0 (NCH$_2$*C*(*p*-tol)$_2$), 67.76 (N*C*H$_2$C(*p*-tol)$_2$), 63.3 (*C*H$_2$Ph), 20.5 (CH_3 *p*-tol).

Crystal Structure Determination of Complexes 3, 6, 8, 12, 13, and 14. Suitable single crystals were mounted onto glass fibers using the "oil-drop" method. Diffraction data were collected at 100−150 K using a NONIUS Kappa CCD diffractometer with graphite-monochromatized Mo Kα radiation (λ = 0.71073 Å). A combination of ω- and φ-scans was carried out to obtain at least a unique data set. Crystal structures were solved by means of the Patterson method, and remaining atoms were located from difference Fourier synthesis, followed by full-matrix least-squares refinement based on F^2 (programs SHELXS-97 and SHELXL-97).[36] Many hydrogen atoms could be found from the Fourier difference. Carbon-bound hydrogen atoms were placed at calculated positions and forced to ride on the attached carbon atom. The hydrogen atom contributions were calculated but not refined. All non-hydrogen atoms were refined with anisotropic displacement parameters. The locations of the largest peaks in the final difference Fourier map calculation as well as the magnitude of the residual electron densities were of no chemical significance. The cell of **6** was found to contain one pentane molecule of crystallization, that of **8** one benzene molecule, that of **12** two benzene molecules, and that of **14** one toluene molecule. Crystal data and details of data collection and structure refinement are given in Table 1. Crystallographic data are also available as cif files (see Supporting Information).

Line Shape Analysis and NMR Simulations. NMR spectral simulations were performed using "gNMR" (Cherwell Scientific). Simulations of the NC*HH*CMe$_2$, NCH$_2$C*Me*$_2$, and ZrC*HH*Ph hydrogens of **8** and NC*HH*CMe$_2$ and NCH$_2$C*Me*$_2$ hydrogens of **13** were performed in a two-step procedure. First, the chemical shifts observed in the slow limit exchange (below 240 K) were used to set up the spin systems. The relative population ratio was fixed at 1:1:3:3:1:1 for **8** and 1:1:3:3 for **13**. The natural line-width in the absence of exchange (W_0 = 2.5 Hz for **8**, 2.6 Hz for **13**) was measured for the Me hydrogens at 250 K. The chemical shifts of the different hydrogens vary slightly in the slow limit exchange, and a linear extrapolation was used to estimate the chemical shifts at higher temperatures. We checked that the observed and calculated chemical shifts for the collapsed resonances are identical. Then, for different temperatures, the exchange rate was varied to get the best fit between the simulated and the experimental spectra; for each complex, all spin systems were processed simultaneously. Activation parameters were determined by a standard Eyring analysis, and the standard deviations from the least-squares fit were used to estimate the uncertainties in $\Delta H^{\ddagger}$ and $\Delta S^{\ddagger}$.[37]

Ethylene Polymerization. Polymerization experiments (Table 8) were performed in a 150 or 320 mL high-pressure glass reactor equipped with a mechanical stirrer and externally heated with a double mantle with a circulating oil bath as desired. In a typical experiment, the reactor was filled with toluene (25 or 70 mL, depending on the size of the reactor) and MAO (30 wt % solution in toluene, 2−3 or 6−8 mL, 500 equiv) or Al*i*Bu$_3$ (0.5−0.8 mL, 10 equiv) and pressurized at 5 atm of ethylene (Air Liquide, 99.99%). The reactor was thermally equilibrated at the desired temperature for 1 h. Ethylene pressure was decreased to 1 atm, and the catalyst precursor (30−50 or 120−150 μmol) in toluene (5 or 10 mL) was added by syringe. The ethylene pressure was immediately increased to 5 atm, and the solution was stirred for the desired time. Ethylene consumption was monitored using an electronic manometer connected to a secondary 100 mL ethylene tank, which feeds the reactor by maintaining constant the total pressure. The polymerization was stopped by venting of the vessel and quenching with a 10% HCl solution in methanol (30 or 80 mL). The polymer was collected by filtration, washed with methanol and acetone (2 × 20 mL), and dried under vacuum overnight.

Acknowledgment. This work was supported by the Ministère de la Recherche et de l'Enseignement Supérieur (Ph.D. grant to L.L.) and the Centre National de la Recherche Scientifique (ATIPE fellowship to J.F.C.). We gratefully thank Dr. Ian Steele (The University of Chicago) for the X-ray crystal diffraction analysis of **8**, and Prof. Richard F. Jordan (The University of Chicago) for GPC analyses and valuable discussions.

Supporting Information Available: Crystallographic data for **3**, **6**, **8**, **12**, **13**, and **14** in CIF format; additional VT ^{1}H NMR data for **5** and **14**; representative GPC and DSC profiles of polyethylenes prepared. This material is available free of charge via the Internet at http://pubs.acs.org

OM0505817

(36) (a) Sheldrick, G. M. *SHELXS-97*, Program for the Determination of Crystal Structures; University of Goettingen: Germany, 1997. (b) Sheldrick, G. M. *SHELXL-97*, Program for the Refinement of Crystal Structures; University of Goettingen: Germany, 1997.

(37) (a) Bevington, P. R. *Data Reduction and Error Analysis for the Physical Sciences*; McGraw-Hill: New York, 1969. (b) Skoog, D. A.; Leary, J. J. *Principles of Instrumental Analysis*, 4th ed.; Saunders College, 1992; pp 13−14.